T F A

ACTA FACULTATIS TECHNICAE

TECHNICAL UNIVERSITY IN ZVOLEN

1

ISSUE: XXX ZVOLEN 2025

Medzinárodný zbor recenzentov / International Reviewers Board

TABLE OF CONTENTS

SCIENTIFIC PAPERS

SCIENTIFIC PAPERS

SAMPLING TECHNIQUES FOR BRAKE WEAR AEROSOLS: A SYSTEMATIC REVIEW

SPÔSOBY ODBERU AEROSÓLU GENEROVANÉHO Z OPOTREBOVANIA BŔZD: SYSTEMATICKÝ PREHĽAD

Janka Szabová[1], Jozef Salva[2], Miroslav Dado[1]

[1]*Department of Manufacturing Technology and Quality Management, Faculty of Technology, Technical University in Zvolen, Študentská 26, 960 01 Zvolen, Slovakia, xszabova@is.tuzvo.sk, dado@tuzvo.sk*
[2]*Department of Environmental Engineering, Faculty of Ecology and Environmental Sciences, Technical University in Zvolen, T. G. Masaryka 24, 960 01 Zvolen, Slovakia, xsalvaj@is.tuzvo.sk,*

ABSTRACT: Brake wear is a significant source of non-exhaust particulate matter (PM) emissions, contributing to air pollution in urban environments and posing potential health risks due to its high content of metals and fine particles. Accurate sampling of brake wear aerosols is essential for quantifying their impact and informing regulatory measures. However, the diversity of sampling approaches and lack of standardized protocols complicate comparisons across studies and hinder the development of effective mitigation strategies. This systematic review aims to identify, classify, and critically assess the sampling techniques used for brake wear aerosols in peer-reviewed research published between 2015 and 2025. Literature searches were conducted using databases Scopus and Web of Science, with inclusion criteria focusing on empirical studies that describe specific sampling methodologies for brake wear particles. Forty-three studies met the criteria and were analysed based on sampling environment, collection mechanism, particle size range, and associated analytical methods. The review highlights the strengths and limitations of each technique, particularly in terms of accuracy, reproducibility, and practical deployment.

Key words: sampling, non-exhaust emission, brake wear particles,

ABSTRAKT: Opotrebenie bŕzd je významným zdrojom nevýfukových emisií tuhých častíc (PM), ktoré prispievajú k znečisteniu ovzdušia v mestskom prostredí a predstavujú potenciálne zdravotné riziká. Korektný odber vzoriek aerosólov z opotrebovania bŕzd je nevyhnutný pre kvantifikáciu ich vplyvu a tvorbu účinných regulačných opatrení. Rôznorodosť prístupov k odberu vzoriek a absencia štandardizovaných protokolov však sťažujú porovnávanie medzi jednotlivými štúdiami a brzdia rozvoj efektívnych stratégií zmierňovania. Cieľom tohto systematického prehľadu je identifikovať, klasifikovať a kriticky zhodnotiť techniky používané na odber aerosólov z opotrebenia bŕzd v recenzovaných vedeckých štúdiách publikovaných v období rokov 2015 až 2025. Vyhľadávanie literatúry bolo uskutočnené v databázach Scopus a Web of Science, pričom do prehľadu boli zahrnuté len experimentálne štúdie opisujúce konkrétne metodiky odberu častíc z bŕzd. Do analýzy bolo zaradených 43 štúdií, ktoré boli analyzované podľa prostredia odberu, metódy odberu vzoriek, veľkostného rozsahu častíc a použitých analytických metód. Prehľad poukazuje na silné a slabé stránky jednotlivých techník, najmä z hľadiska presnosti, reprodukovateľnosti a praktickej využiteľnosti.

Kľúčové slová: odber vzorky, nevýfukové emisie, častice z opotrebenia bŕzd

INTRODUCTION

Air pollution remains one of the most pressing environmental and public health challenges worldwide. Among the various sources of atmospheric particulate matter (PM), traffic-related emissions have been a significant focus of both regulatory and scientific attention. While substantial progress has been made in reducing tailpipe (exhaust) emissions through advances in engine technology and fuel standards, non-exhaust emissions - those not originating from fuel combustion - have been unregulated until now. The Euro 7 emissions standard includes new regulations not just for tailpipe emissions but also for non-exhaust emissions, including brake wear particles and tire wear. Within this category, brake wear particles represent a major and growing concern, particularly in densely populated urban areas

with high vehicular traffic. The regulation introduces a limit of 7 $mg.km^{-1}$ of brake particle emissions for passenger cars and vans. The Euro 7 regulation is expected to take effect in 2027.

Brake wear particles are generated through mechanical abrasion and thermal degradation of friction materials during braking. A comprehensive evaluation of wear particle toxicity necessitates consideration of multiple physicochemical parameters, including particle size distribution, agglomeration state, chemical composition, specific surface area, surface chemistry, and electrostatic charge. Among these, particle size and chemical composition are generally regarded as the primary determinants of toxicological impact (Grigoratos and Martini 2015). One of the challenges in understanding and mitigating the impacts of brake wear emissions lies in their accurate sampling and characterization. The nature of brake wear particles - especially their rapid dispersion, variable composition, and size distribution - makes them particularly difficult to capture and quantify.

Previous reviews (e.g. Piscitello et al. 2021, Wagner et al. 2024, Christou et al. 2025) have addressed non-exhaust emissions broadly, often including tire and road wear or resuspended dust, but few studies have focused specifically and systematically on the sampling techniques used for brake wear particles. Existing reviews and experimental studies typically focus on emission quantification or particle characterization, often treating sampling as a secondary methodological detail. There remains a knowledge gap regarding the strengths and weaknesses of different methods, their suitability under various conditions, and how they influence the interpretation of particulate data. To the best of our knowledge, no previous systematic literature review has been undertaken to above mentioned problematic.

This systematic review seeks to address that gap by providing a comprehensive evaluation of current sampling techniques for brake wear aerosols. The paper answers the following research question: Which sampling methods have been used to study brake wear aerosols, and how do these techniques differ in terms of sampling environment, collection mechanism, temporal resolution, and overall performance? The primary objectives of this study are to:

1. Identify the sampling methods that have been used in peer-reviewed studies on brake wear emissions published between 2015 and 2025.
2. Classify these methods based on sampling environment, collection mechanism, and temporal resolution.
3. Assess the performance characteristics of each technique in terms of accuracy, reproducibility, ease of deployment, and integration with analytical methods.

In doing so, this review aims to support a more coherent and unified approach to the study of brake wear aerosols. Establishing best practices for sampling is a crucial step toward enabling meaningful comparisons across studies, improving the quality of emissions data, and ultimately informing effective air quality management strategies. This is particularly important as policymakers and researchers look beyond tailpipe emissions in their efforts to tackle urban air pollution and its associated health impacts.

The review is structured as follows: Section 2 details the methodology used to identify and select relevant studies, including search strategies, inclusion/exclusion criteria, and data extraction procedures. Section 3 presents the classification and comparative analysis of identified sampling techniques. Section 4 discusses the implications of these findings for research and policy, with a focus on methodological harmonization and future challenges. Finally, Section 5 summarizes the conclusions and key recommendations arising from the review.

In sum, this work contributes to the growing body of literature on non-exhaust emissions by focusing specifically on the technical and methodological aspects of brake wear aerosol sampling. This systematic review provides the first structured synthesis focused specifically on sampling methodologies, integrating evidence from peer-reviewed literature published over

past decade. By systematically identifying, classifying, and assessing the performance of different sampling approaches, this study offers a comparative framework for understanding the methodological strengths, limitations, and contextual suitability of current techniques. By synthesizing the existing evidence, it offers a valuable resource for environmental scientists, engineers, policymakers, and health researchers concerned with the accurate measurement and mitigation of traffic-related particulate emissions.

MATERIAL AND METHODS

This systematic review was conducted in accordance with the PRISMA 2020 guidelines (Page et al. 2021), which provide a standardized approach for identifying, selecting, and critically appraising relevant studies, as well as collecting and analysing data. The study selection process is illustrated in Figure 1.

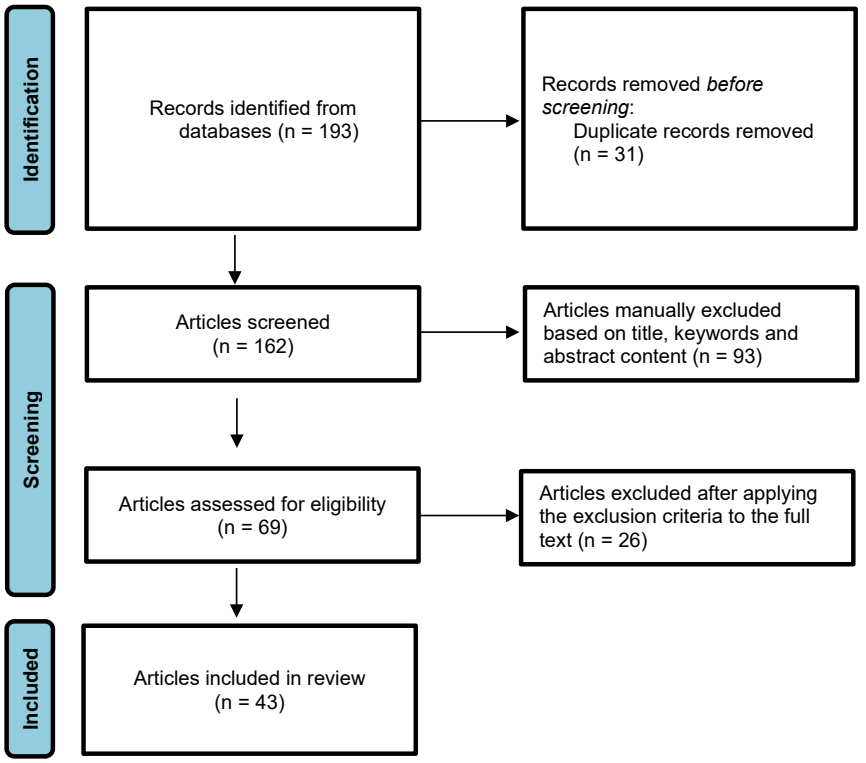

Fig. 1 Flow diagram of studies selection
Obr. 1 Vývojový diagram výberu článkov

Studies were included based on the following predefined eligibility criteria:

- Study Design: Original research articles, including experimental studies.
- Language: Articles published in English.
- Publication Date: Studies published between 2015 and 2025.
- Outcomes: Sampling methodologies and instrumentations for capturing and characterizing brake wear particles.

- Exclusion Criteria: Reviews, editorials, conference abstracts, and studies not reporting any of the above outcomes were excluded.

A systematic search was performed in the electronic databases Scopus and Web of Science. The search strategy was developed using keyword combinations related to "sampling method", and "brake wear" (exact search syntax: "sampling method" AND ("brake" OR "wear"). The study selection process is illustrated in Figure 1. A standardized data extraction form was developed and piloted. The following data were collected from each study:

- Author(s), year, and country.
- Sampling technique or device used.
- Sampling environment.
- Particle size range, mass or number concentration.
- Chemical analysis methods (if any).
- Reported limitations or performance evaluations.

Although formal quality scoring was not performed due to the methodological heterogeneity of engineering-based studies, each study was assessed for reporting completeness, sampling validity, and potential sources of bias (e.g., sampling losses, environmental interference, measurement artifacts). Quantitative meta-analysis was not performed due to lack of standardization in reported outcomes.

RESULTS

An overview of reviewed studies of brake wear particles (BWP) measurement is given in Table 1.

Table 1 Overview of reviewed studies of brake wear particle measurement
Tabuľka 1 Prehľad preskúmaných štúdií merania častíc z opotrebovania bŕzd

Reference	Particle generation method	Measuring device	Type of system
Alemani et al. (2015)	Pin-on-disc tribometer	ELPI+, OPS 3330	Closed
Hagino et al. (2016)	Brake dynamometer	Impactor, DustTrak II	Closed
Verma et al. (2016)	Pin-on-disc tribometer	ELPI+	Closed
Nosko and Oloffson (2017)	Pin-on-disc tribometer	FMPS 3091, OPS 3330, ELPI+, TEOM 1400	Closed
Wahlström et al. (2017)	Pin-on-disc tribometer	ELPI+, OPS 3330, CPC 3772	Closed
Chasapidis et al. (2018)	Chassis dynamometer	CPC 3755, ELPI	Open
Mathissen et al. (2018)	On-road direct measurement, Brake dynamometer	ELPI+	Closed
Perricone et al. (2018)	Pin-on-disc tribometer, Brake dynamometer	ELPI+	Closed
Farwick zum Hagen et al. (2019)	On-road direct measurement	APS 3321, DustTrak 8533, EEPS 3090	Closed
Liati et al. (2019)	Brake dynamometer	DLPI	Closed
Perricone et al. (2019)	Brake dynamometer	ELPI+, HT ELPI+	Closed
Riva et al. (2019)	Brake dynamometer	ELPI+	Closed
Beji et al. (2020)	Chassis dynamometer, On-road direct measurement	CPC, ELPI+, FMPS	Closed
Hascoët and Adamczak (2020)	Brake dynamometer, On-road direct measurement	CPC, ELPI+	Semi-closed
Philippe et al. (2020)	Pin-on-disc tribometer	CNC, ELPI	Closed
Tarasiuk et al. (2020)	Pin-on-disc tribometer	SMPS NanoScan 3910, OPS 3330	Closed
Woo et al. (2021)	Brake dynamometer	APS 3321, FMPS 3091, DustTrak DRX, QCM	Closed

Hesse et al. (2021)	Brake dynamometer	Impactor, CPC 3772, ELPI	Closed
Oroumiyeh and Zhu (2021)	On-road direct measurement	DustTrak 8532, APS 3321	Open
Park et al. (2021)	Brake dynamometer	ELPI+	Closed
Song et al. (2021)	Krauss-type tribometer	OPC Grimm 1.109	Closed
Vojtíšek-Lom et al. (2021)	Brake dynamometer	Cascade impactor, EEPS, ELPI	Closed
Belkacem et al. (2022)	On-road direct measurement	OPC Grimm 1.108	Open
Ghouri et al. (2022)	Brake dynamometer	ELPI+	Closed
Huber et al. (2022)	Brake dynamometer	APC, CPC	Closed
Liu et al. (2022)	Brake dynamometer	ELPI+	Closed
Mamakos et al. (2022)	Brake dynamometer	PM-sampler, APC, CPC	Closed
Men et al. (2022)	Brake dynamometer	Impactor, ELPI+	Closed
Woo et al. (2022)	Brake dynamometer	APS 3321, CPC 3755, ELPI	Closed
Bondorf et al. (2023)	Chassis dynamometer	OPS 3330, CPC 3752, EEPS 3090, ELPI+	Closed
Eggenschwiler et al. (2023)	Chassis dynamometer	Impactor, CPC 3010	Closed
Hamatschek at al. (2023)	Brake dynamometer	ELPI+	Closed
Lyu et al. (2023)	Pin-on-disc tribometer	FMPS 3091, ELPI+	Closed
Storch et al. (2023)	Brake dynamometer	Cascade impactor, CPC 3722, ELPI+	Closed
Vasiljevič et al. (2023)	Brake dynamometer	OPC	Closed
Wang et al. (2023)	Chassis dynamometer	ELPI+, AVL, OBS-ONE	Closed
Andersson et al. (2024)	On-road direct measurement, Chassis dynameter	ELPI+, Horiba MEXA 2000 SPCS	Closed
Hagino (2024)	Brake dynamometer	Impactor LP-20, CPC 3750, FMPS 3091, APS 3321	Closed
Kupper et al. (2024)	Wheel and suspension test bed	CPC 3775, APS 3321, DMA 3081	Closed
Zhang et al. (2024)	Brake dynamometer	ELPI+, APS 3321	Closed
Al Wasir-Ruif (2025)	On-road direct measurement	EEPS 3090	Semi-closed
Neukirchen et al. (2025)	Brake dynamometer	CPC with catalytic stripper, OPS LAP 322, DMS 500	Closed
Yin et al. (2025)	Chassis dynamometer, Brake dynamometer	APS 3321	Closed

BWP sampling techniques can be broadly classified based on sampling environment, sampling mechanism, and temporal resolution (Table 2). Laboratory techniques include dynamometer tests, tribometers, and controlled sampling setups. These allow precise control over braking parameters such as speed, load, and temperature, ensuring reproducibility. Laboratory setups facilitate direct collection of particles from brake systems without interference from other sources. This control enables to isolate brake wear contributions from other particulate sources. Chassis and brake dynamometers simulate real-world braking cycles under laboratory conditions. Field-based techniques include on-vehicle sampling systems, roadside monitoring, and tunnel studies. These methods capture ambient particles in real traffic environments, incorporating effects of varying traffic density, weather, and vehicle types. Field measurements are essential to evaluate actual exposure levels and to validate emission inventories used in air quality models.

Table 2 Classification of Sampling Techniques
Tabuľka 2 Klasifikácia spôsobov odberu vzorky

Category	**Techniques/Instruments**	**Description**
A. Sampling Environment		

□ Laboratory-based	- Pin-on-disc tribometer	The tribometer is generally placed inside a closed box where ambient air is pumped by a fan through a filter.
	- Krauss-type tribometer	It is based on the Krauss test procedure, originally developed for quality control and performance assessment of automotive brake linings.
	- Inertial dynamometer	Inertial dynamometer allows reproducible studies under controlled test conditions.
	- Chassis dynamometer	A chassis dynamometer simulates real-world driving conditions by allowing a full vehicle to be driven stationary, while its wheels rotate on rollers.
□ Field-based	- On-vehicle sampling system	It collects emissions directly from the brake assembly during real-world driving or controlled track tests.
	- Tunnel studies	It estimates BWP emissions by measuring changes in particulate concentration and composition between the entrance and exit of a road tunnel, using chemical tracers to differentiate sources
	- Roadside monitoring	Measuring instruments are placed close to the roadway - especially at locations with frequent braking, like intersections or downhill slopes.
B. Collection Mechanism		
□ Gravimetric	- Filter	It involves drawing air containing particles through a filter medium to collect them for subsequent mass measurement and chemical analysis.
□ Optical	- Photometer	It measures BWP by detecting the light scattered or absorbed by airborne particles in real-time as air passes through an optical chamber.
	- Optical Particle Counter (OPC)	It samples BWP by drawing air through a laser beam and counting particles based on the light they scatter, providing size-resolved particle number concentrations in real time.
	- Condensation Particle Counter (CPC)	It samples BWP by enlarging ultrafine particles through condensation of a working fluid, making them detectable as they pass through an optical sensor for real-time total particle number counting.
	- Aerodynamic Particle Sizer (APS)	It samples BWP by accelerating them through an aerodynamic nozzle and measuring their time-of-flight to determine real-time particle size and concentration.

□ Electrical mobility	- Scanning Mobility Particle Sizer (SMPS)	It samples BWP by classifying them based on their electrical mobility in a differential mobility analyzer and counting them with a condensation particle counter to provide size-resolved particle number distributions.
	- Fast Mobility Particle Sizer (FMPS)	It samples BWP by rapidly classifying particles according to their electrical mobility and simultaneously measuring size-resolved number concentrations in real time.
	- Engine Exhaust Particle Sizer (EEPS)	It samples BWP by electrically classifying particles based on their mobility and providing rapid, real-time size-resolved number distributions across a wide size range.
□ Inertial separation	- Cyclone separator	It samples BWP by using centrifugal force to remove larger particles from an airflow, allowing only particles below a certain aerodynamic diameter to pass through for analysis.
	- Nozzle impactor	It samples BWP by directing an aerosol-laden airflow through a nozzle, causing particles above a specific size to impact onto a collection surface while smaller particles follow the airflow for downstream analysis.
	- Cascade impactor	It samples BWP by sequentially directing airflow through multiple stages with decreasing cut-off sizes, causing particles to impact and collect on separate substrates according to their aerodynamic diameter for size-resolved analysis.
	- Electrical Low Pressure Impactor (ELPI)	It samples BWP by electrically charging airborne particles, separating them by aerodynamic size through low-pressure impaction stages, and measuring their real-time number and size distribution via electrical current detection.
□ Resonance	- Tapered Element Oscillation Microbalance (TEOM)	It samples BWP by collecting them on a filter attached to a vibrating element, where the change in oscillation frequency is used to determine the real-time mass of the deposited particles.
	- Quartz Crystal Microbalance (QCM)	It samples BWP by measuring the change in resonance frequency of a quartz crystal as particles accumulate on its surface, allowing real-time detection of particle mass with high sensitivity.
C. Temporal resolution		
□ Off-line	- Scanning Electron Microscopy with Energy Dispersive X-Ray Spectroscopy (SEM-EDX)	It analyzes BWP by imaging their surface morphology at high resolution and identifying their elemental composition through X-ray emission induced by an electron beam.

	- Inductively Coupled Plasma-Mass Spectrometry (ICP-MS) - Inductively Coupled Plasma-Atomic Emission Spectrometry (ICP-AES)	It analyzes BWP by ionizing digested particle samples in a plasma torch and detecting their elemental composition with high sensitivity based on mass-to-charge ratios. It analyzes BWP by exciting atoms in an acid-digested sample using a high-temperature plasma and measuring the light they emit at characteristic wavelengths to determine their elemental composition.
Real-time	- Real-time monitor	It provides instantaneous data on number concentration and size distribution.

Table 3 presents a comparative analysis of the identified sampling techniques using the following rating scale: limited, low, moderate, high, very high, and excellent.

Table 3 Comparative Analysis of Sampling Techniques
Tabuľka 3 Komparatívna analýza techník odberu vzoriek

Sampling Technique	Accuracy	Reproducibility	Ease of Deployment	Integration with Analytical Methods
Filter Sampling	Moderate to High (dependent on flow control and filter quality)	High – standardized protocols allow consistent results	Moderate – require stationary setup and periodic filter changes	Excellent – filter compatible with gravimetric, SEM-EDX, ICP-MS, and other offline analysis
Cyclone separator	Moderate – effective for coarse particle removal but less precise for ultrafines	High when flow rates are maintained consistently	High – relatively simple and robust devices	Limited standalone use - usually combined with other samplers or instruments downstream
Cascade Impactor	High – size-resolved sampling allows detailed size fractionation	High – stage-by-stage collection reproducible under controlled flow	Moderate to Low – bulky, requires precise flow control and maintenance	Excellent – stages collected on substrate compatible with SEM, gravimetry, and chemical analysis
Photometer	Moderate – mass estimated influenced by particle optical properties and composition	High – under controlled conditions	Very High – compact and easy to deploy	Limited – no size and chemical data: used for real-time mass trend monitoring
APS	Moderate – limited detection for ultrafine particles: accuracy depends on proper calibration	High – provides consistent size distribution and concentration data under controlled and stable sampling conditions	Moderate – portable and capable of real-time measurement, but requires careful sample condition and stable flow control to ensure reliable data	Good - can be integrated with offline chemical analysis (e.g., filters, SEM, ICP-MS) for compositional characterization; requires coordinated sampling protocols
ELPI	High – real-time size resolved number concentration	Moderate – sensitive to operational parameters and particle charge states	High – portable and real-time capable	Good – can be paired with filter sampling for chemical analysis, limited direct chemical data
OPC	Moderate – size and count estimates can be influenced by particle optical properties	High – stable performance under consistent conditions	Very high – compact, portable, and easy to operate	Limited – no direct chemical analysis: often used with complementary sampling
CPC	High for total particle number concentration (especially ultrafines)	High – reproducible number counts if calibration maintained	Very High – portable and user-friendly	Limited – no chemical information, but used with other samplers for full characterization

SMSP	Very High – excellent size resolution and counting accuracy	High – reliable size distributions when stable conditions maintained	Moderate – instrument size and scan time limit field portability	Excellent – size distributions combined with offline chemical analysis possible
FMPS/EEPS	High – real-time size distributions with good resolution	Moderate – requires regular calibration and maintenance	High – smaller and more portable than SMPS	Moderate – size data valuable but chemical analysis requires separate sampling
TEOM	Moderate – mass concentration sensitive, but low ultrafine sensitivity	High – consistent oscillation frequency measurements	Moderate – portable but requires power and stable conditions	Limited – no size or chemical data: often paired with other techniques
QCM	High sensitivity for mass changes	High – stable frequency response if environmental conditions controlled	Moderate – similar to TEOM, requires controlled setup	Limited – no size or chemistry: used as complementary measurement

DISCUSSION

Brake wear aerosols have emerged as a significant source of non-exhaust particulate matter emissions from road traffic, garnering increased scientific and regulatory attention in recent years. This systematic review provides a comprehensive overview of the sampling techniques employed to characterize brake wear aerosols. The importance of accurate and representative sampling cannot be overstated, given that brake wear particles contribute substantially to ambient PM concentrations and have potential adverse effects on human health and the environment.

The review reveals a broad spectrum of sampling techniques utilized in the literature, reflecting the complex nature of brake wear aerosol generation and characterization. Instrumentation plays a central role in shaping our understanding of brake wear aerosols, influencing every step from particle detection to data interpretation. Techniques range from traditional filter-based gravimetric sampling to sophisticated real-time monitoring instruments, often supplemented by chemical and morphological analyses. Filter-based gravimetric sampling remains a foundational approach for collecting brake wear particles, enabling quantification of mass concentration. Commonly, PM is collected on filters, followed by weighing to determine mass load. While this approach offers high accuracy for mass concentration, it lacks temporal resolution and particle size distribution information, limiting its usefulness for understanding dynamic emission patterns. To overcome temporal resolution limitations, many studies employed real-time aerosol monitors, such as optical particle counters (OPCs), condensation particle counters (CPCs), and electrical mobility analyzers like the scanning mobility particle sizer (SMPS). These instruments provide rapid measurement of particle number concentration and size distribution, critical for capturing transient events and variations in brake wear emissions during different driving conditions. However, real-time instruments typically infer mass from number and size data using assumptions about particle density and shape, which can introduce uncertainty given the heterogeneous nature of brake wear particles. A major challenge highlighted across the reviewed studies is the inconsistency in instrument calibration practices. Different instruments are often calibrated using spherical latex particles or standard dust (e.g., Arizona Test Dust), which do not replicate the physical or chemical characteristics of brake wear particles. This leads to systematic biases, particularly in instruments that rely on electrical mobility, light scattering, or inertial separation. Additionally, particle losses due to diffusion, impaction, or electrostatic effects in instrument inlets or tubing systems further compound these uncertainties. Several studies incorporated cascade impactors or micro-orifice uniform deposit impactors (MOUDI) to obtain size-segregated samples, allowing for detailed analysis of particle size distributions in terms of aerodynamic diameter. Size segregation is particularly important because particle size influences deposition patterns

in the respiratory tract and environmental transport. Results consistently indicate that brake wear aerosols are enriched in fine (PM2.5) and ultrafine (<0.1 μm) particle fractions, which are of high relevance for human health due to their deep lung penetration. Most sampling techniques were complemented by chemical analyses, including inductively coupled plasma mass spectrometry (ICP-MS) and scanning electron microscopy coupled with energy dispersive X-ray spectroscopy (SEM-EDS). These methods enable identification of brake wear-specific elemental markers such as copper, antimony, barium, and iron, which are often used to distinguish brake wear aerosols from other traffic-related particles. Morphological analysis further reveals distinctive irregular shapes and fractal structures, aiding source apportionment efforts. Given that no single instrument can provide a complete picture of brake wear aerosols, many studies are shifting toward multimodal sampling strategies, integrating real-time, gravimetric, and chemical instrumentation into cohesive sampling systems.

The reviewed studies exhibit substantial heterogeneity in sampling setups, including differences in sampling height, distance from emission sources, and environmental conditions (e.g., wind speed, temperature, humidity). Sampling locations range from laboratory brake dynamometer chambers to roadside environments with complex emission mixtures. This variability significantly impacts the representativeness of collected samples and the extrapolation of findings to real-world scenarios. One notable finding is the predominance of laboratory or controlled environment sampling setups over field-based techniques. While controlled experiments enable isolation of brake wear emissions from other sources, they may not fully replicate real-world conditions such as varying traffic patterns, meteorological influences, or road surface types. Field studies, though logistically more challenging, provide valuable contextual data but often face difficulties in source apportionment and standardization.

A key limitation identified in the reviewed literature is the lack of consensus on standardized sampling protocols, which hinders cross-study synthesis and meta-analysis. Parameters such as sampling height, distance from the source, and particle size cut-offs vary widely, influencing reported aerosol characteristics. Moreover, temporal variability in brake wear emissions, influenced by driving behaviour and brake system conditions, is often insufficiently accounted for. UN GTR No. 24 (UN 2023) represents a pivotal advancement in the harmonization of non-exhaust emission measurement protocols. UN GTR No. 24 applies exclusively to light-duty vehicles equipped with friction braking systems, including conventional hydraulic brakes and regenerative braking systems when applicable. The regulation excludes heavy-duty vehicles and non-friction brake types (e.g., electromagnetic brakes), which may be addressed in future revisions. The addendum specifies the use of brake dynamometers designed to replicate real braking conditions, controlling parameters such as brake pressure, speed, and temperature. The dynamometer must be capable of reproducing standard braking profiles, including deceleration rates, to simulate urban stop-and-go and highway braking scenarios. A critical element is the sampling system used to capture brake wear aerosols. The addendum prescribes the use of:

- Dilution tunnels or chambers to cool and dilute emissions, mimicking atmospheric conditions and preventing particle agglomeration or evaporation.
- Isokinetic sampling probes to ensure representative particle capture without size-dependent sampling biases.
- Pre-conditioning systems to remove volatile organic compounds and gaseous interferences prior to particulate measurement.

The addendum lays the foundation for extending brake emission measurement to other vehicle classes, integrating on-road testing, and refining chemical characterization methods. Continuous improvements in instrumentation sensitivity and miniaturization are expected to

enhance the precision and applicability of brake wear aerosol measurements in the coming years.

CONCLUSION

This systematic review highlights substantial progress in sampling techniques for brake wear aerosols but also reveals critical challenges that limit the comparability and applicability of current data. Methodological diversity, lack of standardization, and environmental complexity contribute to uncertainties in quantifying brake wear emissions and assessing exposure risks.

Addressing these challenges through harmonized protocols, integrated sampling strategies, and expanded field research will be essential for advancing the understanding of brake wear aerosols and their impacts. Such efforts will ultimately support effective regulatory interventions aimed at reducing non-exhaust traffic emissions and protecting public health.

To advance methodological consistency and improve data reliability in brake wear aerosol studies, several specific recommendations can be proposed based on the findings of this review:

- develop and adopt standardized sampling protocols,
- report complete methodological metadata,
- integrate real-world validation with controlled experiments.

The insights gained here underscore the multifaceted nature of brake wear aerosol sampling and provide a roadmap for future research and policy development. Continued collaboration across disciplines will be vital to develop robust, scalable methodologies that reflect real-world conditions and contribute meaningfully to air quality management.

ACKNOWLEDGMENT

This work was supported by Slovak Research and Development Agency under the Contract no. VV-MVP-24-0227.

REFERENCES

AL WASIF-RUIZ, T., SUÁREZ-BERTA, R., SÁNCHEZ-MARTÍN, J. A., and BARRIOS-SÁNCHEZ, C. C. 2025. Direct measurement of brake wear particles from a light-duty vehicle under real-world driving conditions. In *Environmental Science and Pollution Research,* vol. 32, pp. 2551-2560. DOI:10.1007/s11356-024-35879-y.

ALEMANI, M., NOSKO, O., METINOZ, I., and OLOFSSON, U. 2015. A Study on Emission of Airborne wear Particles from Car Brake Friction Pairs. In *SAE International Journal of Materials and Manufacturing,* no.1, vol. 9, pp. 147-157. DOI:10.4271/2015-01-2665.

ANDERSSON, J., KRAMER, L. J., CAMPBELL, M., MARSHALL, I., NORRIS, J., SOUTHGATE, J., DE VRIES, S., and WAITE, G. 2024. A Practical Approach for On-Road Measurements of Brake Wear Particles from a Light-Duty Vehicle. In *Atmosphere*, vol. 15*,* no. 2. DOI:10.3390/atmos15020224.

BEJI, A., DEBOUDT, K., KHARDI, S., MURESAN, B., FLAMENT, P., FOURMENTIN, M., and LUMIERE, L. 2020. Non-exhaust particle emissions under various driving conditions: Implications for sustainable mobility. In *Transportation Research Part D: Transport and Environment*, vol. 81. DOI:10.1016/j.trd.2020.102290.

BELKACEM, I., HELALI, A., KHARDI, S., and SLIMI, K. 2022. Investigations on vehicle non-exhaust particle emissions: real-time measurements. In *International Journal of Environmental Science and Technology*, vol. 19, pp. 11749-11762. DOI:10.1007/s13762-022-03955-w.

BONDORF, L., KÖHLER, L., GREIN, T., EPPLE, F., PHILIPPS, F., AIGNER, M., and SCHRIPP, T. 2023. Airborne Brake Wear Emissions from a Battery Electric Vehicle. In *Atmosphere*, vol. 14, no. 3. DOI:10.3390/atmos14030488.

CHASAPIDIS, L., GRIGORATOS, T., ZYGOGIANNI, A., TSAKIS, A., and KONSTANDOPOULOS, A. G. 2018. Study of Brake Wear Particle Emissions of a Minivan on a Chassis Dynamometer. In *Emission Control Science and Technology*, vol. 4, pp. 271-278. DOI:10.1007/s40825-018-0105-7.

CHRISTOU, A., GIECHASKIEL, B., OLOFSSON, U., and GRIGORATOS, T. 2025. Review of Health Effects of Automotive Brake and Tyre Wear Particles. In *Toxics*, vol. 13, no. 4. DOI:10.3390/toxics13040301.

DIMOPOULOS EGGENSCHWILER, P., SCHREIBER, D., and HABERSATTER, J. 2023. Brake Particle PN and PM Emissions of a Hybrid Light Duty Vehicle Measured on the Chassis Dynamometer. In *Atmosphere*, vol. 14, no. 5. DOI:10.3390/atmos14050784.

FARWICK ZUM HAGEN, F. H., MATHISSEN, M., GRABIEC, T., HENNICKE, T., RETTING, M., GROCHOWICZ, J., VOGT, R., BENTER, T. 2019. On-road vehicle measurements of brake wear particle emissions. In *Atmospheric Environment*, vol. 217. DOI: 10.1016/j.atmosenv.2019.116943.

GHOURI, I., BARKER, R., BROOKS, P., KOSARIEH, S., and BARTON, D. 2022. The Effects of Corrosion on Particle Emissions from a Grey Cast Iron Brake Disc. In *SAE Technical Paper*. DOI: 10.4271/2022-01-1178.

GRIGORATOS, T. and MARTINI, G. 2015. Brake wear particle emissions: a review. In *Environmental Science and Pollution Research*, vol. 22, pp. 2491-2504. DOI:10.1007/s11356-014-3696-8.

HAGINO, H. 2024. Feasibility of Measuring Brake-Wear Particle Emissions from a Regenerative-Friction Brake Coordination System via Dynamometer Testing. In *Atmosphere*, vol. 15, no. 1. DOI:10.3390/atmos15010075.

HAGINO, H., OYAMA, M., and SASAKI, S. 2016. Laboratory testing of airborne brake wear particle emissions using a dynamometer system under urban city driving cycles. In *Atmospheric Environment*, vol. 131, pp. 269-278. DOI:10.1016/j.atmosenv.2016.02.014.

HAMATSCHEK, C., AUGSBURG, K., SCHOBEL, D., GRAMSTAT, S., STICH, A., GULDEN, F., and HESSE, D. 2023. Comparative Study on the Friction Behaviour and the Particle Formation Process between a Laser Cladded Brake Disc and a Conventional Grey Cast Iron Disc. In *Metals*, vol. 13, no. 2. DOI:10.3390/met13020300.

HASCOËT, M. and ADAMCZAK, L. 2020. At source brake dust collection system. In *Results in Engineering*, vol. 5. DOI: 10.1016/j.rineng.2019.100083.

HESSE, D., HAMATSCHEK, C., AUGSBURG, K., WEIGELT, T., PRAHST, A., and GRAMSTAT, S. 2021. Testing of Alternative Disc Brakes and Friction Materials Regarding Brake Wear Particle Emissions and Temperature Behavior. In *Atmosphere*, vol. 12, no. 4. DOI: 10.3390/atmos12040436.

HUBER, M. P., FISCHER, P., MAMAKOS, A., STEINER, G., and KLUG, A. 2022. Measuring Brake Wear Particles with a Real-Driving Emissions Sampling System on a Brake Dynamometer. In *SAE Technical Paper.* DOI:10.4271/2022-01-1180.

KUPPER, M., SCHUBERT, L., NACHTNEBEL, M., SCHRÖTTNER, H., HUBER, M. P., FISCHER, P., and BERGMANN, A. 2024. Measurement and Analysis of Brake and Tyre Particle Emissions from Automotive Series Components for High-Load Driving Tests on a Wheel and Suspension Test Bed. In *Atmosphere*, vol. 15, no. 4. DOI:10.3390/atmos15040430.

LIATI, A., SCHREIBER, D., LUGOVYY, D., GRAMSTAT, S., and EGGENSCHWILER, P. D. 2019. Airborne particulate matter emissions from vehicle brakes in micro- and nano-scales: Morphology and chemistry by electron microscopy. In *Atmospheric Environment*, vol. 212, pp. 281-289. DOI:10.1016/j.atmosenv.2019.05.037.

LIU, Y., WU, S., CHEN, H., FEDERICI, M., PERRICONE, G., LI, Y., LV, G., MUNIR, S., LUO, Z., and MAO, B. 2022. Brake wear induced PM_{10} emissions during the world harmonised light-duty vehicle test procedure-brake cycle. In *Journal of Cleaner Production*, vol. 361. DOI: 10.1016/j.jclepro.2022.132278.

MAMAKOS, A., HUBER, M., ARNDT, M., REINGRUBER, H., STEINER, G., and WEIDINGER, CH. 2022. Design of a Laboratory Sampling System for Brake Wear Particle Measurements. In *SAE Technical Paper*. DOI: 10.4271/2022-01-1179.

MATHISSEN, M., GROCHOWICZ, J., SCHMIDT, CH., VOGT, R., FARWICK ZUM HAGEN, F. H., GRABIEC, T., STEVEN, H., and GRIGORATOS, T. 2018. A novel real-world braking cycle for studying brake wear particle emissions. In *Wear*, vol. 414-415, pp. 219-226. DOI: 10.1016/j.wear.2018.07.020.

MEN, Z., ZHANG, X., PENG, J., ZHANG, J., FANG, T., GUO, Q., WEI, N., ZHANG, Q, WANG, T., WU, L., and MAO, H. 2022. Determining factors and parameterization of brake wear particle emission. In *Journal of Hazardous Materials*, vol. 434. DOI: 10.1016/j.jhazmat.2022.128856.

NEUKIRCHEN, C., BOZORGZAD, M., MÄDER, M., BECKER, J., BUCCHIANICO, S., TRAPP, CH., ZIMMERMANN, R., and ADAM, T. 2025. Comprehensive elemental and physical characterization of vehicle brake wear emissions from two different brake pads following the Global Technical Regulation methodology. In *Journal of Hazardous Materials*, vol. 482. DOI:10.1016/j.jhazmat.2024.136609.

NOSKO, O. and OLOFSSON, U. 2017. Effective density of airborne wear particles from car brake materials. In *Journal of Aerosol Science*, vol. 107, pp. 94-106. DOI: 10.1016/j.jaerosci.2017.02.014.

OROUMIYEAH, F. and ZHU, Y. 2021. Brake and tire particles measured from on-road vehicles: Effects of vehicle mass and braking intensity. In *Atmospheric Environment:X*, vol. 12. DOI:10.1016/j.aeaoa.2021.100121

PAGE, M. J. et al. 2021. The PRISMA 2020 statement: an updated guideline for reporting systematic reviews. In *BMJ*, vol. 372, no. 71. DOI:10.1136/bmj.n71.

PARK, J., JOO, B., SEO, H., SONG, W., LEE, J. J., LEE, W. K., and JANG, H. 2021. Analysis of wear induced particle emissions from brake pads during the worldwide harmonized light vehicles test procedure (WLTP). In *Wear*, vol. 466-467. DOI:10.1016/j.wear.2020.203539.

PERRICONE, G., MATĚJKA, V., ALEMANI, M., VALOTA, G., BONFANTI, A., CIOTTI, A., OLOFSSON, U., SÖDERBERG, A., WAHLSTRÖM, J., NOSKO, O., STRAFFELINI, G.,

GIALANELLA, S., and IBRAHIM, M. 2018. A concept for reducing PM_{10} emissions for car brakes by 50%. In *Wear,* vol. 396-397, pp. 135-145. DOI:10.1016/j.wear.2017.06.018.

PERRICONE, G., MATĚJKA, V., ALEMANI, M., WAHLSTRÖM, J., and OLOFSSON, U. 2019. A Test Stand Study on the Volatile Emissions of a Passenger Car Brake Assembly. In *Atmosphere*, vol. 10, no. 5. DOI:10.3390/atmos10050263.

PHILIPPE, F., XIANG, M., MORGENEYER, M., CHEN, Y., CHARLES, P., GUINGAND, F., and BRESSOT, CH. 2020. Emission rate assessment of airborne brake particles by characterization of the pad and disc surfaces from a pin-on-disc tribometer. In *Toxicology Research and Application*, vol 4. DOI:10.1177/2397847320977782.

PISCITELLO, A., BIANCO, C., CASASSO, A., and SETHI, R. 2021. Non-exhaust traffic emissions: Sources, characterization, and mitigation measures. In *Science of the Total Environment*, vol. 766. DOI:10.1016/j.scitotenv.2020.144440.

RIVA, G., VALOTA, G., PERRICONE, G., and WAHLSTRÖM, J. 2019. An FEA approach to simulate disc brake wear and airborne particle emissions. In *Tribology International*, vol. 138, pp. 90-98. DOI:10.1016/j.triboint.2019.05.035.

SONG, W., PARK, J., CHOI, J., LEE, J. J., and JANG, H. 2021. Effects of reinforcing fibers on airborne particle emissions from brake pads. In *Wear*, vol. 484-485. DOI: 10.1016/j.wear.2021.203996.

STORCH, L., HAMATSCHEK, C., HESSE, D., FEIST, F., BACHMANN, T., EICHLER, P., and GRIGORATOS, T. 2023. Comprehensive Analysis of Current Primary Measures to Mitigate Brake Wear Particle Emissions from Light-Duty Vehicles. In *Atmosphere*, vol. 14, no. 4. DOI:10.3390/atmos14040712.

TARASIUK, W., TSYBRII, Y., and NOSKO, O. 2020. Correlations between the wear of car brake friction materials and airborne wear particle emissions. In *Wear*, vol. 456-457. DOI: 10.1016/j.wear.2020.203361.

VASILJEVIĆ, S., GLIŠOVIĆ, J., MILORADOVIĆ, D., STANOJEVIĆ, M., and DORDEVIĆ, M. 2023. Analysis of Parameters Influencing the Formation of Particles during the Braking Process: Experimental Approach. In *Atmosphere*, vol. 14, no. 11. DOI: 10.3390/atmos14111618.

VERMA, P. CH., ALEMANI, M., GIALANELLA, S., LUTTEROTI, L., OLOFSSON, U., and STRAFFELINI, G. 2017. Wear debris from brake system materials: a multi-analytical characterization approach. In *Tribology International*, vol. 94, pp. 249-259. DOI: 10.1016/j.triboint.2015.08.011.

VOJTÍŠEK-LOM, M., VACULÍK, M., PECHOUT, M., HOPAN, F., ARUL RAJ, A. F., HORÁK, J., POPOVICHEVA, O., ONDRÁČEK, J., and DOUŠOVÁ, B. 2021. Effects of braking conditions on nanoparticle emissions from passenger car friction brakes. In *Science of the Total Environment*, vol. 788. DOI: 10.1016/j.scitotenv.2021.147779.

WAGNER, S., FUNK, CH. W., MÜLLER, K., and RAITHEL, D. J. 2024. The chemical composition and sources of road dust, and of tire and road wear particles – A review. In *Science of the Total Environment*, vol. 926. DOI: 10.1016/j.scitotenv.2024.171694.

WAHLSTRÖM, J., LYU, Y., MATĚJKA, V., and SÖDERBERG, A. 2017. A pin-on-disc tribometer study of disc brake contact pairs with respect to wear and airborne particle emissions. In *Wear*, vol. 384-385, pp. 124-130. DOI: 10.1016/j.wear.2017.05.011.

WANG, Y., LI, J., YIN, H., YANG, Z., ZHONG, CH., SUN, J., HU, Y., LI, Z., SHAO, Y., ZHANG, L., DU, T., and GE, Y. 2023. A new method to assess vehicle airborne non-exhaust

particles: Principle, application and emission evaluation. In *Applied Energy*, vol. 352. DOI: 10.1016/j.apenergy.2023.121942.

WEI, L., CHOY, Y.S., and CHEUNG, C.S. 2023. The effect of braking conditions on the particular matter emissions and brake squeal. In *Wear*, vol. 530-531. DOI: 10.1016/j.wear.2023.205045.

WOO, S. H., JANG, H., NA, M. Y., CHANG, H. J., and LEE, S. 2022. Characterization of brake particles emitted from non-asbestos organic and low-metallic brake pads under normal and harsh braking conditions. In *Atmospheric Environment*, vol. 278. DOI: 10.1016/j.atmosenv.2022.119089.

WOO, S. H., KIM, Y., LEE, S., CHOI, Y., and LEE, S. 2021. Characteristics of brake wear particle (BWP) emissions under various test driving cycles. In *Wear*, vol. 480-481. DOI: 10.1016/j.wear.2021.203936.

YIN, J., XU, Z., WEI, W., JIA, Z., FANG, T., JIANG, Z., CAO, Z., WU, L., WEI, N., MEN, Z., GUO, Q., ZHANG, Q., and MAO, H. 2025. Laboratory measurement and machine learning-based analysis of driving factors for brake wear particle emissions from light-duty electric vehicles and heavy-duty vehicles. In *Journal of Hazardous Materials*, vol. 488. DOI: 10.1016/j.jhazmat.2025.137433.

ZHANG, Q., YIN, J., FANG, T., GUO, Q., SUN, J., PENG, J., ZHONG, CH., WU, L., and MAO, H. 2024. Regenerative braking system effectively reduces the formation of brake wear particles. In *Journal of Hazardous Materials*, vol. 465. DOI:10.1016/j.jhazmat.2023.133350.

Corresponding author:
Ing. Janka Szabová, e-mail: xszabova@is.tuzvo.sk

USE OF AN IMU FOR DETECTING POSITIONAL DEVIATIONS OF A PRESS SLIDE FOR ROBOTIC TRAJECTORY CORRECTION

MOŽNOSTI VYUŽITIA INERCIÁLNEHO SENZORA NA DETEKCIU POLOHOVÝCH ODCHÝLIEK LISU PRE KOREKCIU TRAJEKTÓRIE PRIEMYSELNÉHO ROBOTA

Roman Čierťažský[1], Elena Pivarčiová[2]

[1]*KVAT, FT, TUZVO, T.G. Masaryka 2117/24, 960 01, Zvolen, SR, roman.ciertazsky@tuzvo.sk*
[2]*KVAT, FT, TUZVO, T.G. Masaryka 2117/24, 960 01, Zvolen, SR, elena.pivarciova@tuzvo.sk*

ABSTRACT: This research study analyzes the possibilities of adaptive trajectory correction of an industrial robot when removing sand cores from molds (core boxes). The main problem is the translational deviations of the press table slides (Cold Box and Anorganic Box), as well as the ejectors that eject the cores from the mold, which are caused by wear, vibrations, but also by inconsistent sensing of the press positions using inductive sensors when the robot is removing the cores. These phenomena lead to incorrect removal, collisions, and productivity losses. The aim of this work is to evaluate the suitability of inertial measurement units (IMUs) for detecting these press deviations in real time and their use in an adaptive correction system. The study reviews existing sensor approaches (IMUs, optical systems, encoders) with an emphasis on their advantages, limitations, and reliability in a foundry environment. It critically evaluates sensor data fusion methods (Kalman filters) and hybrid solutions for suppressing IMU drift. The conclusion provides recommendations for the implementation of systems that will increase the accuracy, adaptability, and robustness of robotic operations in demanding production conditions.

Key words: adaptive trajectory correction, inertial measurement unit (IMU), sensor data fusion, industrial robot, sand core picking

ABSTRAKT: Táto rešeršná štúdia analyzuje možnosti adaptívnej korekcie trajektórie priemyselného robota pri odbere pieskových jadier z foriem (jadrovníkov). Hlavným problémom sú translančné odchýlky stolových saní lisu (Cold Box a Anorganic Box), taktiež vyhadzovákov vysúvajúcich jadrá z formy, ktoré sú spôsobené opotrebením, vibráciami, ale aj nekonštantným snímaním polôh lisu pomocou indukčných snímačov v stave odoberania jadier robotom. Tieto javy vedú k chybnému odberu, kolíziám a stratám produktivity. Cieľom práce je vyhodnotiť vhodnosť inerciálnych meracích jednotiek (IMU) pre detekciu týchto odchýlok lisu v reálnom čase a ich využitie v systéme adaptívnej korekcie. Štúdia prehliada existujúce senzorické prístupy (IMU, optické systémy, enkodéry) s dôrazom na ich výhody, limity a spoľahlivosť v prostredí zlievarenstva. Kriticky hodnotí metódy fúzie senzorických dát (Kalmanove filtre) a hybridné riešenia na potlačenie driftu IMU. Záver poskytuje odporúčania pre implementáciu systémov, ktoré zvýšia presnosť, prispôsobivosť a robustnosť robotických operácií v náročných výrobných podmienkach.

Kľúčové slová: adaptívna korekcia trajektórie, inerciálna meracia jednotka (IMU), fúzia senzorických dát, priemyselný robot, odber pieskových jadier

INTRODUCTION

Industrial robots are essential in foundries for automating demanding and repetitive tasks, such as removing sand cores (core boxes) from molds after casting. The precise position of the mold/core is critical for successful removal by the robot. In real production conditions, undesirable deviations occur that complicate this process.

The primary cause is **translational deviations of the press slide and ejector plate**, which are caused by wear on the stops, vibrations of the pressing unit, thermal expansion, or inaccuracy of the inductive position sensors. These sensors can be affected by metal surroundings or transient states (TE Connectivity, 2024). In addition, inductive sensors themselves, although robust, can provide unstable data during dynamic motion or at low speeds, precisely at the critical moment of robot picking (ABB, 2023).

The consequences of these deviations lead to:

- incorrect clamping of robot cores by the effector,
- collisions between the robot, effector, and mold/ejector,
- damage to cores, effectors, or molds,
- line stoppages, loss of time, and productivity.

The aim of this study is to critically examine the potential of inertial measurement units (IMUs) as a key sensor for detecting these deviations in real time and the possibility of integrating them into an adaptive robot trajectory correction system, thereby increasing the robustness and adaptability of the entire process.

THE PRESENT STATE OF KNOWLEDGE

The effort to increase the adaptability, accuracy, and robustness of industrial robots is a key pillar of the Industry 4.0 concept. Traditional robot programming, based on the "teach-in" method, where trajectory points are precisely defined in advance, reaches its limits in dynamic and unstructured environments. Real-world manufacturing conditions, characterized by machine wear, thermal expansion, and vibrations, cause deviations that lead to inaccuracies and failures in robotic applications.

To solve these problems, research worldwide is moving towards sensor-controlled adaptive robotics. The dominant approach is the use of external sensor systems, especially optical ones. Systems based on 2D/3D cameras and scanners can measure the position and orientation of an object with high accuracy and provide the robot's control system with data for real-time trajectory correction. For example, Lee and Song (2009) demonstrated a significant reduction in drift through periodic calibration with an industrial camera. However, the disadvantage of these systems is their high sensitivity to environmental conditions—dust, smoke, changes in lighting, or reflections from metal surfaces—which significantly limits their reliability in demanding environments such as foundries (FISA, 2022). It is precisely in the context of environmentally demanding applications, where optical methods fail, that inertial measurement units (IMUs) come into play. The following table summarizes the key differences between optical systems and IMUs in the context of foundry applications.

Table 1 Comparison of optical systems and IMUs (FISA, 2022; Hislop et al., 2021; Lee & Song 2009; Pintér & Božek, 2012; Wang et al., 2012)
Tabuľka 1 Porovnanie optických systémov a IMU (FISA, 2022; Hislop et al., 2021; Lee & Song 2009; Pintér & Božek, 2012; Wang et al., 2012)

Criterion	*Optical systems (2D/3D Cameras)*	*Inertial Measurement Units (IMU)*
Accuracy	High when measuring absolute position and orientation under ideal conditions.	Prone to drift (cumulative error) in long-term absolute position measurement. Excellent for measuring short-term dynamic changes.
Environmental resistance	Very low. Sensitivity to dust, smoke, steam, lighting changes and glare.	High. Independence from visual conditions, resistance to dust and smoke.
Latency	Higher, due to high computational demands.	Very low, provides high frequency data (hundreds to thousands of Hz).
Price and complexity	High price and high computational requirements.	Relatively low price and compact dimensions.
Main use	Suitable for precise calibration or verification in a controlled environment.	Suitable for detecting deviations and vibrations in real time directly at the source.

IMU sensors are an attractive alternative thanks to their compactness, durability, and independence from visual conditions. Their ability to directly measure dynamic changes (acceleration and angular velocity) on the machine body allows them to detect deviations that

are invisible to external sensors. International research confirms the potential of merging data from IMUs and encoders to achieve sub-millimeter accuracy (Trinh et al., 2024).

Overcoming dynamic errors requires sensor technology that provides accurate, high-frequency motion information independently. IMU appears to be a key tool. IMU measures acceleration and angular velocity using accelerometers and gyroscopes, enabling six degrees of freedom motion tracking (6-DoF) (Pintér & Božek, 2012). The advantage of robotic correction is **independence from external references**. IMU does not need external signals and is resistant to interference, which is ideal for industrial environments (Pivarčiová et al., 2018; Pintér & Božek, 2012). Another advantage is **high data frequency**. MEMS sensors provide data at high frequencies (hundreds to thousands of Hz), which is critical for compensating for rapid dynamic phenomena (Hislop et al., 2021; Wang et al., 2012).

The main limitation is **drift**, where the biggest challenge is the accumulation of errors in the integration of measured values, causing the position estimate to gradually deviate from reality. IMU is therefore unsuitable for long-term absolute positioning (Pivarčiová et al., 2018; Qazizada et al., 2016; Hislop et al., 2021, Fourati, 2014). The IMU also limits **noise and Bias**, i.e. sensor outputs are subject to noise and systematic deviations that need to be filtered out (Hislop et al., 2021; Rhudy & Gu, 2013).

Understanding the strengths and limitations of IMUs has led to the development of sophisticated strategies that exploit their ability to measure motion dynamics while attempting to circumvent the problem of drift. IMUs thus become not only sensors, but also powerful calibration tools. The work of Alban and Janocha presents a method of dynamic calibration using an external IMU attached to the end effector. This allows direct measurement of dynamic trajectory deviations. Based on the measured data, an error model is created, which is used in real time to compensate for the desired trajectory. Experimentally, it was possible to reduce the maximum trajectory deviation by 85% (Alban & Janocha, 1999). The work of Hislop et al. (2021) provides quantitative data on the performance limits of commercial IMUs. The orientation estimation error (RMSE) ranged from 0.2° to 12.5°, and the average drift was 0.4° per hour. These results show that IMUs are excellent for measuring short-term dynamic changes, but their absolute estimates quickly become unreliable without external correction.

In Slovakia, too, several academic and research institutions are working on improving the accuracy and adaptability of robots. The work of Pintér and Božek, which has direct relevance to Slovak research, proposes the use of an inertial navigation system (INS) to calibrate the entire robotic workplace (Pintér & Božek, 2012). The goal is not only to correct the robot itself, but to align the entire simulation model of the production equipment with real geometric conditions. František Duchoň (STU in Bratislava) is an expert in mobile and industrial robotics, sensor fusion, and Kalman filters. His research includes the application of Kalman filters to the fusion of data from GNSS and IMU for robot localization (Mikulová et al., 2017). Ivan Kuric (UNIZA in Žilina) focuses on automation, robotics and manufacturing technologies, with his research in the field of real-time robot trajectory correction using a laser tracker being particularly relevant (Kuric et al., 2020). Michal Kelemen and Ivan Virgala (Technical University of Košice) specialize in mechatronics, robot design, control, and sensors. Their work includes the design of specific robotic mechanisms and the analysis of kinematic and dynamic models (Sinčák et al., 2021). Ján Piteľ and Ján Semjon (TU in Košice) (Mižáková et al., 2013; Semjon et al., 2016) focus on automation, robotics, and mechatronics. Piteľ deals with the theory of automatic control and estimation of forces in robot joints, while Semjon focuses on precise positioning mechanisms and kinematics. Dušan Nemec and Viliam Tlach (UNIZA in Žilina) focus on control systems, robotics, artificial intelligence (Nemec) and automation of mechanical engineering production (Tlach). D. Nemec's research includes industrial process control and intelligent systems (Chynoradský & Božek., 2016; Nemec et al., 2017; Čuboňová et al.,b 2021).

This research study therefore focuses on analyzing and comparing methods of sensor data fusion and hybrid architectures aimed at eliminating IMU drift and enabling the development of a robust adaptive robot trajectory correction system specifically for foundry production conditions. While this review draws on several key local Slovak research contributions, it sets their findings within the context of broader international challenges in sensor fusion and robotics.

PROBLEM ANALYSIS

The primary source of deviations are table slides carrying the mold for sand cores and the ejector plate ensuring the stroke of the ejectors to eject the cores from the mold. These are Cold Box (hereinafter referred to as "CB") and Anorganic Box (hereinafter referred to as "AB") presses. Fig. 1 shows the process phase in the state of core removal by a robot, including the names of the individual parts.

Fig. 1 Removing cores from the mold using a robot with an effector
Obr. 1 Odobratie jadier z formy pomocou robota s efektorom

The main characteristics of the deviations are predominantly low-frequency translational shifts in the *X, Y*, and *Z axes* (Fig. 2), in the order of millimeters to centimeters, often combined with low-frequency vibrations. Rotations (roll, pitch, yaw) are usually smaller in magnitude but significant for the orientation of the core. An important factor not detailed in this initial analysis is the total travel length of the slide and the time required for its extension. For the CB press, the typical extension travel is approximately 1200 mm, completed in a cycle time of 4-6 seconds. For the AB press, the travel is shorter, around 800 mm, completed in 3-5 seconds. This information is critical for assessing the suitability of IMUs, as sensor drift is time-dependent and accumulates over the measurement period.

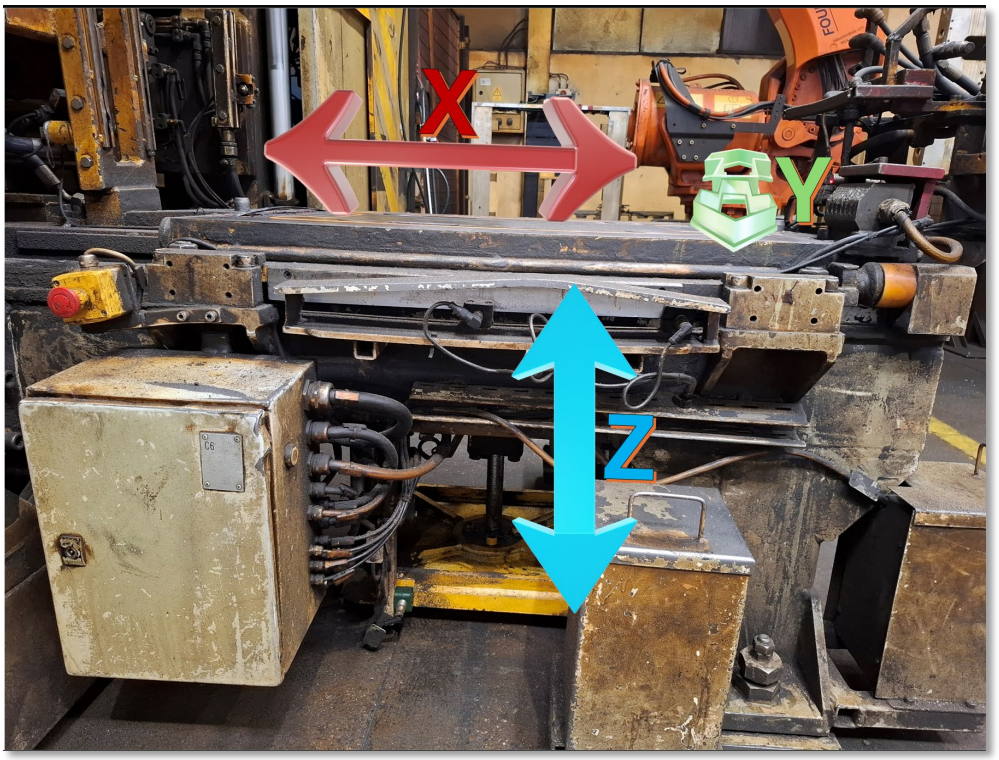

Fig. 2 Displaying the direction of deviation axes
Obr. 2 Zobrazenie smerovania osí odchýliek

Another significant factor contributing to deviations is the influence of the environment. The foundry environment is characterized by high temperatures, dust, metal chips, electromagnetic interference, and strong vibrations from pressing and striking mechanisms (FISA, 2022). Table 2 lists the causes of their occurrence.

Table 2 The table contains the causes of their occurrence, specifically for AB and CB presses
Tabuľka 2 Tabuľka obsahuje príčiny ich vzniku, špecificky pre lisy AB a CB

Deviation in direction	***axes X* and *Y***	***axes X* and *Y***	***axes X* and *Y***	***axes X* and *Y***	***axes X*, *Y* and *Z***	**axis *Z***
Machine:	AB, CB	AB, CB	AB, CB	AB	AB, CB	CB
Cause:	dirty bump stops **Fig. 3 – A**	pinion damage **Fig. 3 – B**	damage to the guide and rails **Fig. 3 – C**	encoder calibration **Fig. 3 – D**	Corebox change **Fig. 3 – E**	changing the height of the ejector sensor **Fig. 3 – F**

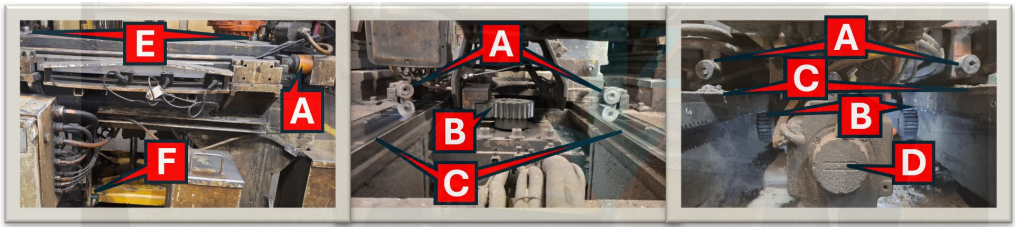

Fig. 3 Deviations on CB (right, centre), on AB (left)
Obr. 3 Odchýlky na CB (vpravo, stred), na AB (vľavo)

MATERIAL AND METHODS

Several sensor technologies can be considered for detecting deviations in table slides and ejector plates. Their comparison is shown in Table 3.

Table 3 Comparison of sensory technologies (ABB, 2023; Aggarwal et al., 2010; FISA, 2022; Hislop et al., 2021; Lee et al., 2009; TE Connectivity, 2024; Pivarčiová et al., 2018)
Tabuľka 3 Porovnanie senzorických technológií (ABB, 2023; Aggarwal et al., 2010; FISA, 2022; Hislop et al., 2021; Lee et al., 2009; TE Connectivity, 2024; Pivarčiová et al., 2018)

Type sensory technologies	Principle	Benefits	Disadvantages/ Limits on Foundry	Suitability for Real Correction
Inductive Sensors	Measuring distance from metal target	Robust, durable, relatively accurate in static condition	Susceptible to EMC interference, inaccuracies at low speeds/motion, only measures position relative to one axis, does not provide orientation	Low –. main source of inaccuracies
Optical Sensors (Cameras, 3D scanners)	Scene visualization, point cloud	High accuracy, full 3D information (position + orientation), flexibility	Very susceptible to dust, smoke, high temperatures, lighting differences, need for clear view, high price, high computational demands	Medium – suitable for calibration/verification, less so for real-world correction due to environment and latency
Laser Distance Sensors (LIDAR, ToF)	Measuring the time of flight of light	Good short-range accuracy, less sensitive to light than cameras	Sensitive to dust/smoke, reflections from shiny metal surfaces, limited field of view, high price	Medium – similar limitations as optics
Absolute Encoders	Angle/position measurement on an axis	Very high accuracy and resolution, direct measurement method	Mounting only on rotary or linear shafts, prone to contamination, higher price, complicated installation on existing machines	Medium/High – excellent for accurate measurement of sled movement if installable, but does not provide vibration/orientation
Inertial Measurement Unit (IMU)	Acceleration (accelerometer) and angular velocity (gyroscope) measurement	Compact, relatively inexpensive, measure movement directly on the mounting surface (slide/extender), do not require external infrastructure/view, measure vibrations, suitable for dynamic measurement	Drift (cumulative error over time), sensitivity to high-frequency vibrations and shocks, sensitivity to temperature changes, need for fusion with other data for absolute position/orientation	High – for detecting relative deviations from the expected trajectory in real time, especially in combination

Note: This table provides a comparative overview. A more detailed implementation study would require citing specific datasheets for each sensor model considered.

Inertial Measurement Units (IMU)

IMU combines a typical three-axis accelerometer and a three-axis gyroscope. MEMS (Micro-Electro-Mechanical Systems) technology prevails in industrial applications. To use IMU for deviation detection, the following principles must be applied (Groves 2013):

1. **Installation:** the IMU is attached directly to the moving part of the core box – the ejector plate (one sensor = detection of all 3 axes, both the slide and the ejectors). Fig. 4 shows the location of the sensor.

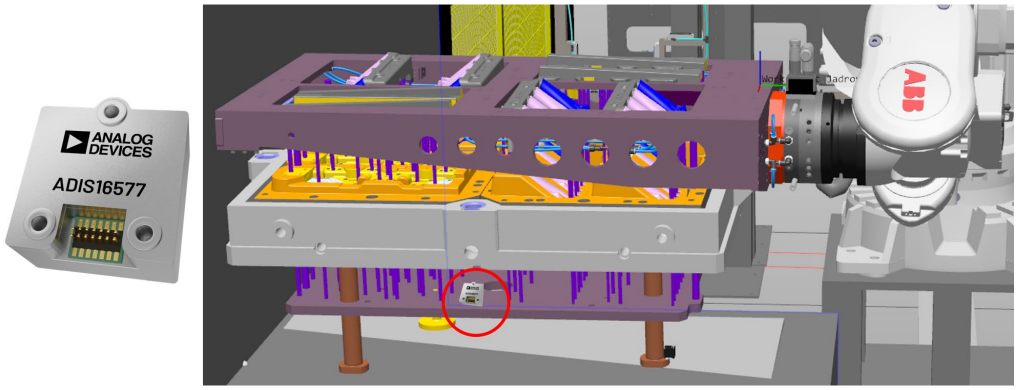

Fig. 4 IMU sensor (left) (Analog Device 2024), Sensor location (right)
Obr. 4 IMU senzor (vľavo) (Analog Device 2024), Umiestnenie senzora (vpravo)

2. **Reference recording:** with the known, precise position of the press (calibration), the expected inertial profile (acceleration, angular velocity) for its movement to the sampling position is recorded.
3. **Real measurement:** the actual inertial profile is measured during each cycle.
4. **Deviation detection:** The difference between the expected and measured profiles indicates a deviation. Double integration of acceleration (accelerometer) over time gives the displacement (*Δx*, *Δy*, *Δz*). Integration of angular velocity (gyroscope) gives the rotation (*Δroll*, *Δpitch*, *Δyaw*).

Calculation example of displacement from acceleration (simplified 1D):

$$\Delta v = \int a(t)\ dt \quad (1)$$

$$\Delta s = \int v(t)\ dt = \iint a(t)\ dt^2 \quad (2)$$

where

Δv is the change in speed [m.s^{-1}],
Δs is the shift – critical for detecting translational deviation [m],
a(t) is the measured acceleration – after subtracting gravity and the expected profile [m.s^{-2}].

Note: The equations above represent a simplified model. In real-world implementation, it is necessary to take into account the initial conditions (speed and position at the start of integration) and perform the correct transformation between the coordinate systems of the press and the robot, which is part of thorough system calibration.

- The key advantages for the application are:
  - **Direct measurement at the source of the deviation:** eliminates errors caused by mechanical connections or external scanning.

- **High sampling frequency:** (>100 Hz) enables the capture of rapid vibrations and dynamic transient phenomena (BOSCH 2023).
- **Independence from external conditions:** works in dust, smoke, low light conditions, without the need for visibility.
- **Compactness and durability:** modern MEMS IMUs are suitable for industrial environments.
- **Vibration measurement:** helps diagnose the condition of the press (wear, loosening).

➢ Main challenge: **Drift and its sources** (Aggarwal et al., 2010)**:**

- **Sensor Bias (offset):** A small constant error in the measurement of acceleration or angular velocity. Fig. 5 shows a graph depicting the actual position (straight line) and the calculated position from the IMU (wavy and gradually deviating) over time – demonstrating the rapid growth of the error.
  For gyro: ω_meas = ω_true + β_gyro + noise. The integration of β_gyro leads to a linearly increasing angle.
  For accelerometer: a_meas = a_true + β_acc + noise. Double integration of β_acc leads to a quadratically increasing position error.

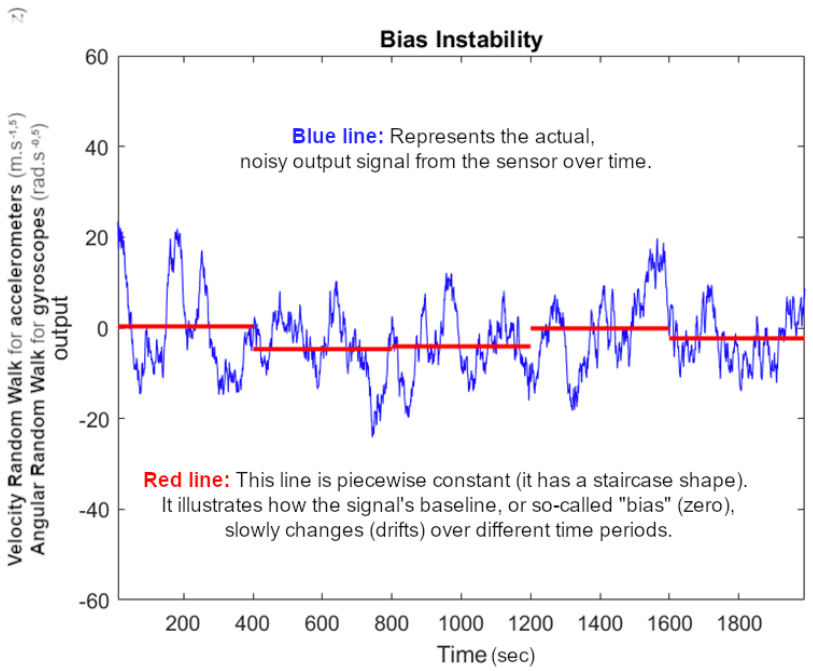

Fig. 5 Typical position drift from double integration of IMS accelerometer acceleration (without correction) (SBG 2024)
Obr. 5 Typický drift pozície od dvojitej integrácie zrýchlenia IMS akcelerometra (bez korekcie) (SBG 2024)

- **Sensor noise:** random noise during integration leads to random walk of position/angle.
- **Nonlinearity and scaling factors:** imperfect sensor response.

- **Temperature effects:** variations in ambient temperature, especially in a foundry, significantly alter sensor Bias and scale factors, representing a primary source of drift (STMicroelectronics 2024). This influence must be actively compensated for.
- **Vibrations:** may cause false acceleration detections (vibro-interruption) or sensor saturation.

Sensor data fusion and IMU drift suppression

A pure IMU solution is not sufficient for long-term stable detection of absolute position deviation due to drift. Sensor fusion with other sources of information is necessary.

- Types of complementary sensors:
  - **Absolute encoders** (if it is possible to install)**:** They provide highly accurate and drift-free information about the position/angle of the sled or ejector plate in their own axis. An ideal source for correcting IMU drift in the same axis (Trinh et al. 2024).
  - **Magnetometers (Part of IMU):** measure the direction of the Earth's magnetic field. They can help correct drift in the yaw angle. Severely limited in foundries: Large metal objects and electric currents significantly distort the magnetic field, causing large errors (Kok et al. 2017, Li & Vala 2019).
  - **Temperature Sensors:** given the significant impact of temperature on IMU bias, a dedicated temperature sensor (either integrated into the IMU module or placed nearby) is essential. Its data can be fed into the fusion algorithm (e.g., an EKF) to model and compensate for thermal drift in real-time.
  - **External reference points (Optical/Laser):** highly accurate position measurement via cameras or laser trackers directed at reflective targets on the sled/ejector plate. Can be used for periodic IMU drift correction, but not in real time due to latency and environmental issues (Lee & Song 2020).

- Fusion methods:
  - **Kalman Filters (KF) and their variants**: mathematical framework for optimal state estimation (position, velocity, orientation, sensor Bias) based on the system model and sensor noise characteristics (Kalman 1960):
    - **Linear Kalman Filter (KF):** for linear systems and Gaussian noise.
    - **Extended Kalman Filter (EKF):** most used. Linearizes nonlinear models (such as IMU motion equations) around the current estimate (Welch & Bishop 2006; Solá 2017; Thrun at al. 2005).
    - **Non - invasive Kalman Filter (UKF):** uses a deterministic sampling approach to better handle nonlinearities, computationally more demanding.
    - **Complementary Filter:** a simpler alternative for merging gyro and accelerometer/magnetometer for orientation estimation (e.g. Madgwick, Mahony). Less suitable for merging with position. (Madgwick 2011).

- Hybrid architectures for foundries:
  - **IMU + Absolute encoder** (if available): Kalman fusion with an encoder eliminates drift in the motion axis. Trinh et al. (2024) achieved an accuracy of 0 % to 1.48 % when measuring linear displacement in industrial conditions using a fusion of MEMS IMU and a high-resolution encoder.
  - **IMU + Periodic Optical Calibration:** the industrial camera system (Intel RealSense D435) corrected IMU drift every 10 cycles, reducing position error from 20 mm to 1.5 mm in an environment with metal debris (Lee et al., 2009)

Table 4 Comparison of fusion methods (Lee et al., 2009)
Tabuľka 4 Porovnanie metód fúzie (Lee et al., 2009)

Method	RMSE of position [mm]	Latency [ms]	Dust resistance
Only IMU	15,8	2	High
IMU + Encoder (EKF)	0,3	5	Medium
IMU + Optical Calibration	1,2	120	Low

DISCUSSION

The analysis presented indicates that an IMU-based system is a viable solution for the specific problem of press slide deviation. However, its successful implementation hinges on a robust system architecture, which must address data processing, communication, and the practical method of correction.

1. **Data Processing and Fusion:** An IMU sensor module (ideally combined with an encoder and temperature sensor) would feed raw data to a local data fusion processor (e.g., an embedded PC or microcontroller).This processor is the core of the solution. It would run an Extended Kalman Filter (EKF) or a similar fusion algorithm, as discussed. This algorithm must not only fuse IMU data with a secondary source (like an encoder or temperature sensor) but also actively estimate and correct for the time-varying sensor biases. The reference trajectory data would serve as the predictive model for the filter, with the IMU measuring the deviation from this prediction.
2. **Communication with Supervisory Computer:** The calculated deviation (ΔP) must be transmitted to the robot controller or a supervisory PLC reliably and with minimal, deterministic latency. Standard industrial protocols such as EtherCAT or PROFINET IRT (with latency < 5ms) are essential for this, as a non-deterministic delay (e.g., over standard TCP/IP) would render the correction useless (Beckhoff, 2024). The data packet would contain the 6-DoF correction vector (Δx, Δy, Δz, Δroll, Δpitch, Δyaw).
3. **Time synchronization** (e.g., via IEEE 1588 PTP) between the sensor system and the robot controller is critical to ensure the measured deviation corresponds precisely to the robot's position in its own execution cycle (Gaderer et al., 2010).
4. **Adaptive controller:** An adaptive controller in the robot or PLC would then adjust the target trajectory based on the received deviation **ΔP** Fig. 6.

```python
def adjust_trajectory(P_target, ΔP):
    P_corrected = P_target + ΔP
    if np.linalg.norm(ΔP) > MAX_DEVIATION:
        trigger_safety_stop()  # Bezpečnostná poistka
    return P_corrected
```

Fig. 6 Trajectory adjustment algorithm
Obr. 6 Algoritmus upravujúci trajektóriu)

- Methods of correction:
  - **Shift of the target point (TCP):** this is the most direct method. The correction is applied directly to the coordinates of the end effector at the target pickup point. This approach is ideal for compensating for simple translational deviations, where the entire target point has shifted without changing orientation.

- **Shift in the target framework:** with this method, the correction is applied to the reference frame in which the trajectory is defined, which can affect multiple points along the path. This method is more suitable for more complex deviations that involve not only displacement but also rotation, and ensures that the entire trajectory of the robot's approach is adjusted to the new position and orientation of the mold.
- **Adaptation via Force Control** (if available): the deviation can serve as input for a force-controlled contact or a gentle touch in the event of incorrect positioning (De Luca & Mattone 2005).

Contribution and Added Value:
The primary contribution of this research is the specific application of IMU-based sensing to a problem (press slide deviation in a foundry) where traditional optical or inductive sensors fail due to environmental harshness or inherent inaccuracy. While IMU drift is a known challenge, this paper argues that for this specific short-duration, cyclical motion (4-6 seconds), the drift can be effectively managed, a concept supported by research into 'zero-velocity updates' (ZUPT) and cyclical motion analysis (Woodman, 2007). The value added is a pathway to a low-cost, high-reliability sensing solution that can be retrofitted to existing machinery, directly reducing collisions, downtime, and material waste. It moves the process from a purely pre-programmed operation to an adaptive one, capable of handling real-world wear and tear.

IMU selection for foundries

Table 5 contains criteria for MEMS IMUs in harsh environments.

Table 5 Criteria for MEMS IMU in foundry (Analog Devices, 2023; Bosch, 2023)
Tabuľka 5 Kritéria pre MEMS IMU v zlievarenstve (Analog Devices, 2023; Bosch, 2023)

Parameter	Minimum requirement	Recommended value
Gyro bias stability	5 °/h	< 1 °/h
Accelerometer noise	150 µg/√Hz	< 80 µg/√Hz
Vibration range	±8 g	±16 g
Protection	IP65	IP67
Operating temperature	–40 °C to +85 °C	–40 °C to +105 °C

Recommended models:

1. **ADI ADIS16507** (for high accuracy): This is a tactical-grade IMU known for its high stability. Gyro Bias stability: 0.8 °/h, VRE: 0.1 mg.g^{-2}. It is often used in aerospace and high-performance robotics where precision is paramount.

2. **Bosch BMI088** (economic choice): This is a high-performance automotive/industrial-grade IMU. Impact resistance 10 000 g, suitable for vibrations. While more cost-effective, it would require more aggressive filtering and thermal compensation compared to a tactical-grade unit. Industrial-grade modules (e.g., Xsens MTi-series): These are fully integrated, pre-calibrated, and temperature-compensated sensor modules. They often come in ruggedized, IP67-rated enclosures and provide a complete data processing pipeline (including on-board sensor fusion and EKF), outputting corrected orientation and acceleration data directly. This simplifies integration and is a common choice for industrial automation.

CONCLUSION

Inertial measurement units (IMUs) represent a very promising technology for detecting translational deviations of the press and ejector plate in real time during the removal of sand cores by a robot. Their main advantages – direct measurement at the source of the deviation, independence from visual conditions, high sampling frequency, and compactness – make them particularly suitable for demanding foundry environments.

The key factor for success is **the effective suppression of drift** inherent in MEMS IMUs. Based on the overview, the following can be recommended:

1. **Hybrid sensor solution:** the combination of IMU with absolute encoders (if their installation on the sled/ejector plate is technically and economically feasible) represents the optimal approach. The encoder provides a drift-free position in its axis, while the IMU adds information about vibrations, lateral movements, and orientation. Fusion using an extended Kalman filter (EKF) is a suitable method.
2. **Alternative in the absence of encoder:** if encoders can't be installed, you should think about doing periodic optical calibration of the IMU. For example, a camera on the robot arm could periodically (e.g., at the beginning of a shift or after a certain number of cycles) measure a reference point on the sled and correct the IMU status (position, Bias). This requires a robust optical system and highlighted reference points.
3. **Emphasis on IMU selection:** the critical parameters of the IMU for this application are low noise, excellent hstability (especially of the gyroscope) and low vibration sensitivity (VRE). Investing in a higher-class MEMS IMU (e.g., tactical/industrial) is worthwhile due to significantly better drift suppression and stability. Active temperature compensation, likely requiring a dedicated temperature sensor input to the fusion algorithm, is non-negotiable.
4. **Robust implementation:** the system must include fast and deterministic communication between the data processing unit on the press and the robot's RCS, as well as precise time synchronization. Safety mechanisms for detecting and handling sensor errors (e.g., saturation, failure) and thorough calibration of the transformation between the coordinate systems of the press and the robot.
5. **Utilization of diagnostic potential:** IMU data (mainly vibrations) should also be monitored for predictive maintenance purposes of the press.

The implementation of an adaptive trajectory correction system based on IMU and data fusion has the potential to significantly increase the reliability of core removal, reduce the number of collisions and downtime, and increase the overall productivity of robotic foundry lines, thereby increasing their autonomy and robustness in demanding production conditions.

Future work should focus on the practical implementation of this system, including the development of a physical testbed, the creation of detailed communication and data processing diagrams, and experimental validation of drift suppression over extended production runs.

ACKNOWLEDGMENT

The article was prepared as part of a grant project KEGA 004TU Z-4/2024: Implementation of progressive methods of education in professional subjects in the field of mechanical engineering and industrial robotics.

REFERENCES

ABB, Core Handling Applications: Common Failure Modes and Sensor Limitations. [online] [cit. 2023-12-31]. Available on: <https://new.abb.com/products/robotics/core-handling/tech-report>.

AGGARWAL, P., SYED, Z., NOURELDIN, A., EL-SHEIMY, N., 2010. MEMS-Based Integrated Navigation. *Artech House.*

ALBAN, G., JANOCHA, H. 1999. Dynamic Calibration of Industrial Robots with Inertial Measurement Systems. In *Proceedings of the 30th ISR (International Symposium on Robotics)*.

ANALOG DEVICES, Vibration Rectification Error in MEMS Accelerometers. [online] [cit. 2023-12-31]. Available on: <https://www.analog.com/en/technical-articles/vibration-rectification-error-in-mems-gyroscopes.html>.

ANALOG DEVICES, ADIS 16577. [online] [cit. 2024-12-31]. Available on: <https://www.analog.com/en/products/adis16577.html>.

BECKHOFF, Automation of EtherCAT - The Ethernet Fieldbus. [online] [cit. 2024-12-31]. Available on: <https://www.beckhoff.com/en-en/ethercat/>.

BOSCH, Sensortec: Application Note: Using IMUs for Vibration Monitoring in Industrial Equipment. [online] [cit. 2023-12-31]. Available on: <https://www.bosch-ensortec.com/media/appnotes/an012_vibration_monitoring.pdf>.

CHYNORADSKÝ, L., BOŽEK, P., 2016. Research and Development of a new System of the Autonomous Control of Robot Trajectory. In *Acta Mechatronica*, no. 1(1), pp 25-28. ISSN 2453-7306.

ČUBOŇOVÁ, N., BULEJ, V., NÁPRSTKOVÁ, N., DODOK, T., TLACH, V., 2021. *Automatizácia strojárskej výroby*. 1. vyd. Žilina: EDIS – vydavateľstvo Žilinskej univerzity. ISBN 978-80-554-1836-0.

DE LUCA, A., MATTONE, R. 2005. Sensorless Robot Collision Detection and Hybrid Force/Motion Control. In *Proceedings of the 2005 IEEE International Conference on Robotics and Automation*, pp 2389-2394. DOI: https://doi.org/10.1109/ROBOT.2005.1570247.

MIKULOVÁ, Z.;DUCHOŇ, F. BABINEC, A., DEKAN, M. 2017. Localization of mobile robot using visual system. In: *International Journal of Advanced Robotic Systems*, no. 14(5). DOI: http://dx.doi.org/10.1177/1729881417736085.

FISA, Environmental Specifications for Automation Systems in Foundries. [online] [cit. 2022-12-31]. Available on: <https://www.foundrystandards.org/fisa-2022>.

FOURATI, H. (ed.), 2014. *Multisensor Data Fusion: From Algorithms and Taught Applications to IMU/GNSS and Camera-IMU Integration*. CRC Press. ISBN 978-1-4665-9839-4.

GADERER, G., LOSCHMIDT, P., SAUTER, T. 2010. Improving Fault Tolerance in High-Precision Clock Synchronization. In *IEEE Transactions on Industrial Informatics*, pp 206-215. DOI: https://doi.org/10.1109/TII.2010.2044580.

GROVES, P.D., 2013. Principles of GNSS, Inertial, and Multisensor Integrated Navigation Systems (2nd ed.). *Artech House.*, ISBN 978-1-60807-005-3.

HISLOP, J., ISAKSSON, M., MCCORMIK, J., HENSMAN, C., 2021. Validation of 3-Space Wireless Inertial Measurement Units Using an Industrial Robot. In *Sensors*, no. 21(20), pp 6858. DOI: https://doi.org/10.3390/s21206858.

KALMAN, R. E., 1960. A New Approach to Linear Filtering and Prediction Problems. In *Journal of Basic Engineering,* no. 82(1), pp 35-45. DOI: http://dx.doi.org/10.1115/1.3662552

KOK, M., HOL, J. D., SCHÖN, T. B., 2017. Using Inertial Sensors for Position and Orientation Estimation. In *Foundations and Trends in Signal Processing*, no. 11(1-2), pp 1-153. DOI: https://doi.org/10.1561/2000000094.

KURIC, I., TLACH, V., CÍSAR, M., SÁGOVÁ, Z., ZAJAČKO, I., 2020. Examination of industrial robot performance parameters utilizing machine tool diagnostic methods. In *International Journal of Advanced Robotic Systems,* no. 17(1). DOI: https://doi.org/10.1177/1729881420905723.

LEE, Y-J., YIM, B-D., SONG, J. B., 2009. Mobile robot localization based on effective combination of vision and range sensors. In *nternational Conference on Intelligent Robots and Systems*, no. 7, pp 97-104. DOI: https://doi.org/10.1007/s12555-009-0112-0. .

LI, Q., VALA, M., 2019. Challenges of IMU-based Orientation Estimation in Ferromagnetic Environments. In *Proceedings of the IEEE International Conference on Mechatronics and Automation (ICMA)*, pp 1120-1125. DOI: 10.1109/ICMA.2019.8816451. Neviem ho stiahnuť

MADGWICK, S. O. H., HARRISON, A. J. L., VAIDYANATHAN, R., 2011. Estimation of IMU and MARG orientation using a gradient descent algorithm. In *IEEE International Conference on Rehabilitation Robotics*, pp 1-7. DOI: https://doi.org/10.1109/ICORR.2011.5975346.

MIŽÁKOVÁ, J., PITEĽ, J., TÓTHOVÁ, M., 2013. Pneumatic Artificial Muscle as Actuator in Mechatronic System. In *Applied Mechanics and Materials*, no. 460, pp 81-90. DOI: https://doi.org/10.4028/www.scientific.net/AMM.460.81.

NEMEC, D., JANOTA, A., GREGOR, M., HRUBOŠ, M., PIRNIK, R. 2017. Control of the mobile robot by hand movement measured by inertial sensors. In *Electrical Engineering*, no. 99(4), pp 1161-1168. Available on: https://link.springer.com/article/10.1007/s00202-017-0614-3

PINTÉR, T., BOŽEK, P. 2012. Industrial Robot Control using Inertial Navigation System. In *Advanced Materials Research*, no. 605-607, pp 1600-1604. DOI: https://doi.org/10.4028/www.scientific.net/AMR.605-607.1600.

PIVARČIOVÁ, E., BOŽEK, P., TURYGIN, J., ZAJAČKO, I., SHCHENYATSKY, A., VÁCLAV, Š., CÍSAR M., GEMELA, B., 2018. Analysis of control and correction options of mobile robot trajectory by an inertial navigation system. In *International Journal of Advanced Robotic Systems*, no 15(1), pp 1-10. DOI: https://doi.org/10.1177/1729881418755165.

QAZIZADA, E. M., PIVARCIOVA, E., 2016. Mobile robot controlling possibilities of inertial navigation system. In *Procedia Engineering*, no. 149, pp 404-413. DOI: https://doi.org/10.1016/j.proeng.2016.06.685.

RHUDY, M., GU, Y., 2013. Understanding Nonlinear Kalman Filters, Part I: Selection between EKF and UKF. In *West Virginia University*. Available on: https://yugu.faculty.wvu.edu/files/d/fed008fa-14a3-48c4-b7b4-cb75b83ea7db/irl_wvu_online_ekf_vs_ukf_v1-0_06_28_2013.pdf.

SBG, IMU, [online] [cit. 2024-12-31]. Available on: https://support.sbg-systems.com/sc/kb/latest/technology-insights/how-to-compare-imu.

SEMJON, J., HAJDUK, M., VARGA, J., JÁNOŠ, R., MARCINKO, P., 2016. Assembly Workplace of Electrical Contacts. In *American Journal of Mechanical Engineering*, no 4(7), pp 258-261. Available on: https://pubs.sciepub.com/ajme/4/7/5/index.html.

SINČÁK, P. J., VIRGALA, I., KELEMEN, M., PRADA, E., BOBOVSKÝ, Z., KOT, T. 2021. Chimney Sweeping Robot Based on a Pneumatic Actuator. Applied Sciences. In *Novus Scientia*, no. 11(11), pp 4872. DOI: https://doi.org/10.3390/app11114872.

SOLÁ, J., 2017. Quaternion kinematics for the error-state Kalman Filter. Available on: https://www.iri.upc.edu/people/jsola/JoanSola/objectes/notes/kinematics.pdf.

STMicroelectronics, AN5108, Temperature Compensation for LSM6DSOX IMU. [online] [cit. 2024-12-31]. Available on: <https://www.st.com/resource/en/application_note/an5108-temperature-compensation-for-lsm6dsox-stmicroelectronics.pdf>.

TE CONNECTIVITY, Harsh Environment Sensor Technologies [online]. [cit. 2024-06-26]. Available on: <https://www.te.com/en/industries/industrial-machinery/insights/five-sensor-technologies.html>.

TRINH, T. K., PHONG, L. T., NHAN, D. K., 2024. Autonomous Mobile Robot Localization by Using IMU and Encoder Data Fusion Technique by Kalman Filter. In *Advances in Engineering Research and Application*, no. 943, pp 245-256. DOI: https://doi.org/10.1007/978-3-031-62238-0_28.

THRUN, S., BURGARD, W., FOX, D., 2005. *Probabilistic Robotics*. MIT Press. ISBN 978-0262201629.

WANG, C., CHEN, W.-H., TOMIZUKA, M., 2012. Robot end-effector sensing with position sensitive detector and inertial sensors. In *IEEE International Conference on Robotics and Automation*. pp 5252-5257. Available on: https://researchwith.njit.edu/en/publications/robot-end-effector-sensing-with-position-sensitive-detector-and-i.

WELCH, G., BISHOP, G. 2006. An Introduction to the Kalman Filter. In *U University of North Carolina at Chapel Hill*. Available on: https://www.cs.unc.edu/~welch/media/pdf/kalman_intro.pdf.

WOODMAN, O. J., 2007. *An introduction to inertial navigation*. University of Cambridge, Computer Laboratory. Technical Report UCAM-CL-TR-696. Available on: https://www.cl.cam.ac.uk/techreports/UCAM-CL-TR-696.pdf.

Corresponding author:
Ing. Roman Čierťažský, tel.: +421 905 908 563, e-mail: roman.ciertazsky@tuzvo.sk

EXPERIMENTAL ANALYSIS OF DESIGNS AND APPLICATIONS OF SOLUTIONS FOR MODIFYING TOOLS FOR MECHANIZING FORESTRY WORK

EXPERIMENTÁLNA ANALÝZA NÁVRHOV A APLIKÁCIÍ RIEŠENÍ PRE ÚPRAVU NÁSTROJOV NA MECHANIZÁCIU LESNÝCH PRÁC

Miroslava Ťavodová

Department of Manufacturing Technologies and Quality Management, Faculty of Technology Technical University in Zvolen, Študentská 26, 960 01 Zvolen, Slovakia, tavodova@tuzvo.sk

ABSTRACT: The article deals with the comparison and evaluation of two hardfacing materials for exposed places of tools for crushing unwanted growths and unconventional material with the original material of tool from the material 16CrMn5. For the evaluation of selected hardfacing materials, electrodes UTP BMC EN 14700 and E DUR 600 EN ISO 14700 were selected. The unconventional material was X120Mn12 – Hadfield steel. Two types of methods were used for testing. For the evaluation of abrasion resistance, the method according to GOST23.208-79 was used. For measuring hardness, the Rockwell method HRC and the microhardness measurement according to Vickers HV0.1 were used. The strengthening of the X120Mn12 material was carried out by intense impacts on the surface to create intense plastic deformation, simulating the loading of the tool in operation. Based on the measurement results, we can conclude that all three selected materials and processes increased both the hardness and abrasion resistance of the surfaces of the tools for crushing unwanted growths. This can be attributed mainly to the given conditions of the structure of the applied materials, mainly due to their chemical composition and the ability to self-reinforce under operating conditions when crushing unwanted growths.

Key words: hardfacing, Hadfield steel, abrasion, hardness, forestry tools

ABSTRAKT: Článok sa zaoberá porovnaním a hodnotením dvoch tvrdonávarových materiálov na exponované plochy nástrojov na drvenie nežiadúcich nárastov a nekonvenčného materiálu s pôvodným materiálom nástroja z materiálu 16CrMn5. Pre hodnotenie vybraných tvdonávarových materiálov boli vybrané elektródy UTP BMC EN 14700 a E DUR 600 EN ISO 14700. Nekonvenčný materiál bol zvolený X120Mn12 – Hadfieldová oceľ. pre testovanie boli využité dva druhy metód. Pre hodnotenie oteruvzdornosti bola použitá metóda podľa GOST23.208-79. Pre meranie tvrdosti Rockwellova metóda HRC a meranie mikrotvrdosti podľa Vickersa HV0.1. Spevnenie materiálu X120Mn12 sa uskutočnilo intenzívnymi rázmi na povrch, aby sa vytvorila intenzívna plastická deformácia, simulujúca zaťaženie nástoja v prevádzke. Na základe výsledkov meraní môžeme konštatovať, že všetky tri zvolené materiály a postupy zvýšili ako tvrdosť tak aj oteruvzdornosť plôch nástrojov na drvenie nežiadúcich nárastov. Je možné to pripísať hlavne daným podmienkam vyhovujúcej štruktúre aplikovaných materiálov, podmienené hlavne ich chemickým zložením ako aj schopnosťou samospevňovania sa v prevádzkových podmienkach pri drvení nežiadúcich nárastov.

Kľúčové slová: tvrdonávar, Hadfieldova oceľ, abrázia, tvrdosť, lesné nástroje

INTRODUCTION

Forests fulfill an important production and public benefit function. Therefore, they need to be sustainably managed. However, this requires mechanization, which is subject to wear and tear over time. The working parts of machines are also exposed to this wear and tear – tools that come into direct contact with the cultivated soil and woody vegetation (Hnilica et al. 2015; Hnilcová et al. 2016). Tools used for environmental modification in forest cultivation and establishment are subjected to high loads in a non-homogeneous working environment during their work. This environment is primarily formed by the processed wood mass, which has an uneven composition and hardness (Falat et al. 2019; Ťavodová et al. 2023). Another important component of this environment is soil. The soil is characterized by the fact that its surface contains unpredictably and irregularly distributed minerals and rocks of different hardness, size

and origin. The high speed of the rotor adapter of the base machine on which the tools are mounted also contributes to the rapid wear of the tools, as well as the uneven loading of individual tools in connection with their mounting on the rotor. The tools themselves are manufactured as composite - the tool body with tips, most often made of sintered carbides, or as monolithic (Ťavodová et al. 2019).

In practice, it often happens that after a certain period of operation, due to the heterogeneity of the environment and the dynamic load on the tool, the tip is lost and the tool body is further worn and deformed. This is caused by the cyclical repetition of the plastic deformation of the microsurface layers of the tool under abrasion conditions, resulting in significant material loss (Zum Gahr, 1998); (Suchánek et al. 2007; Javaheri et al. 2018; Singh et al. 2020). This wear is then very significant after a short time, which leads to the loss of functionality of the tool and its premature removal from service. Frequent tool replacement and frequent and lengthy machine downtimes then cause economic problems for companies operating in forestry (Ťavodová et al. 2023).

Operating conditions represent a whole set of often variable quantities, the change of which leads to a change in the intensity, or even the mechanism of abrasive wear (Buchely et al. 2005; Chotěborský et al. 2009). There are several methods and procedures for increasing the wear resistance of tools. By choosing those that ensure a change in the structure of the tool body that is more resistant to abrasive wear, we can extend its use in operation. This creates the assumption of increasing its service life. This will bring a reduction in costs for operators in forestry (Hnilica et al. 2015; Falat et al. 2019).

MATERIAL AND METHODS

One of the very effective measures that increases wear resistance is hardfacing functional surfaces with a suitable hardfacing material. The hardfacing materials used for this purpose have different properties. When choosing them, it is necessary to consistently base on the method of stressing the hardfaced part and at the same time take into account the composition of the base metal (Balla 2003). The cutting edge of the cutting tools is stressed differently, and the jaws of crushers or mulching tools are stressed differently. Other hardfacing metal materials are suitable for working with sand and gravel, others for tools that work in the soil or process wood (Ťavodová et al. 2019).

For the evaluation of the selected hardfacing materials as well as a new, unconventional material, the following were chosen:

for evaluating the degree of wear of materials

• tests of resistance to abrasive wear according to GOST 23.208-79;

for evaluating the hardness of materials

• Rockwell hardness tests HRC - EN ISO 6508-1;

• microhardness tests according to Vickers HV0.1 - EN ISO 6507.

The measurement was conducted on samples of materials, the characteristics of which are listed in Table 1.

Table 1 Characteristics of materials
Tabuľka 1 Charakteristiky materiálov

Material	Chemical composition[1)]	Hardness[2)]	Microstructure[3)]
Material of body tool Steel 16CrMn5[4)]	C – 0.15%; Mn – 1.25%; Si – 0.27%; Cr - 0.9% Fe – balance[6)]	256 HB 19 HRC	ferrite-pearlite
Electrode UTP BMC EN 14700	C – 0.6%; Si – 0.8%; Mn – 16.5%; Cr – 13.5%; Fe – balance	48-53 HRC	austenite

Electrode E DUR 600 EN ISO 14700	C – 0.7%; Mn – 0.5%; Cr – 10%; Si – 1.9%; Fe - balance	59 HRC	ledeburite
Hadfield´s steel X120Mn12[5)]	C – 1.2%; Si – 0.4%; Mn -13 %; Cr – 1.5%; Fe - balance	Before strengthening – 200HB/19HRC[7)] After strengthening – 600HB/56HRC[8)]	austenite

[1)]Chemické zloženie, [2)]Tvrdosť, [3)]Mikroštruktúra, [4)]Materiál tela nástroja, [5)]Hadfieldova oceľ, [6)]Zvyšok [7)]Pred spevnením, [8)]Po spevnení

The material 16CrMn5 represents a standard. The values obtained from the tests were compared with it to determine whether the selected materials have better or worse properties than the tool body material. The reinforcement of the material X120Mn12 was carried out using intensive impacts on the hardface surface for 2 minutes, to create intense plastic deformation on the PRAKO KAP 40 hammer, with a weight of 40 kg and a maximum stroke of 220 mm. With this, we attempted to simulate the impact loading of the tool in operation.

Fig.1a shows tool for crushing unwanted growths and Fig. 1b prepared of hardfacing specimen with Electrode E DUR 600 (example).

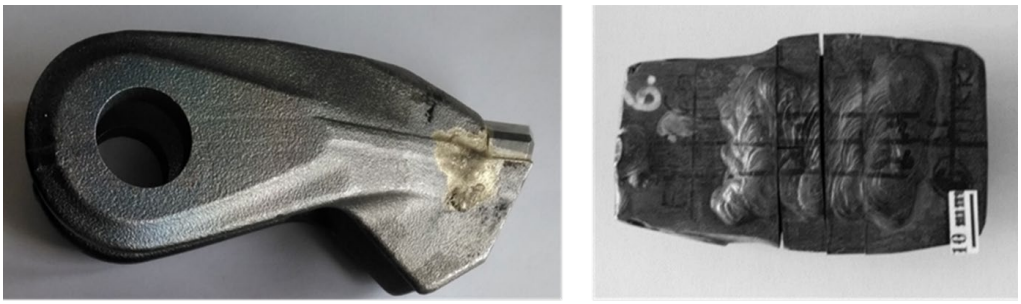

a b

Fig. 1 New tool (a); specimen with hardfacing materials - example Electrode E DUR 600 (b)
Obr. 1 Nový nástroj (a); vzorka s návarom – príklad elektróda E DUR 600 (b)

RESULTS

Evaluation of the wear rate of materials

To determine whether the materials we selected predict better resistance to extreme abrasive and impact loads with their mechanical properties, relevant tests and measurements were performed on samples under laboratory conditions.

The abrasion resistance test was performed on the TESTER T-07 device, ITE PIB along with the device for recording individual cycles BT-16 Controller, ITE PIB (Fig. 1). The dimensions of the samples were 30x30x5 mm. The parameters of the device for abrasion resistance tests are in Table 2.

Table 2 Parameters of the device for abrasion resistance tests
Tabuľka 2 Parametre zariadenia pre skúšku odolnosti voči abrázii

	Parameter	Values [7)]	Units [8)]
1	Number of cycles [1)] c	11	-
2	Length of friction path in one cycle [2)] R	153.6	m
3	Diameter of rubber disc [3)] D	48.9	mm

4	Pressure force [4)] F	15.68	N
5	Disc speed in one cycle [5)] o	1,000	rpm
6	Grain size - silica sand OTTAWA [6)] s_g	0.1	mm

[1)]Počet cyklov, [2)]Dĺžka trecej dráhy v jednom cykle, [3)]Priemer gumového kotúča, [4)]Prítlačná sila, [5)]Rýchlosť kotúča v jednom cykle, [6)]Veľkosť zrna – kremičitý piesok, [7)]Hodnoty, [8)]Jednotky

In Fig. 2a there is a device for testing abrasion resistance. In Fig. 2b there is a schematic of the device with a description, and in Fig. 2c there is a test specimen, sample.

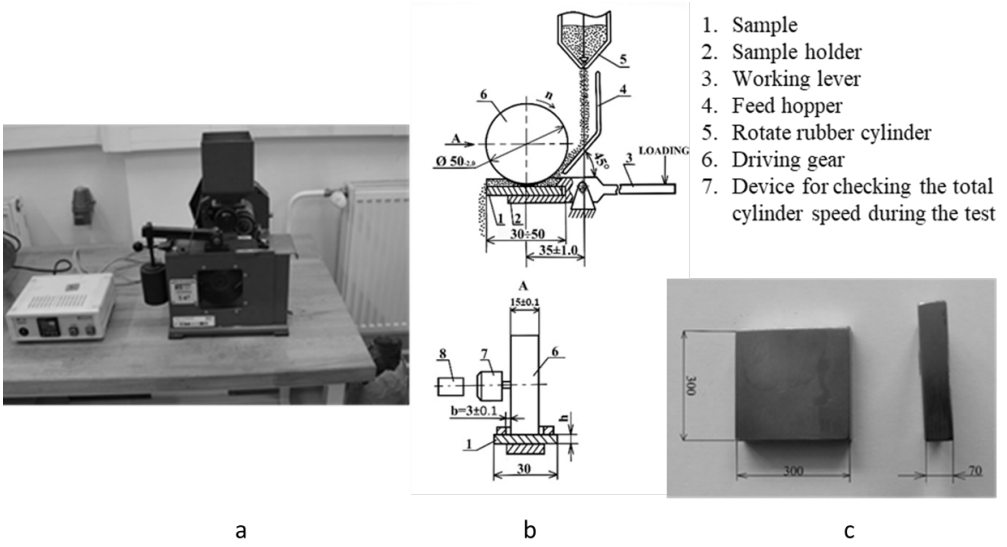

Fig. 2 Device for testing abrasion resistance (a); schematic of the device with a description (b); test sample (c)
Obr. 2 Zariadenie pre skúšku odolnosti voči abrázii (a); schéma s popisom (b); testovacia vzorka (c)

After each cycle, the sample was taken and weighed 3 times in order to determine the material's weight loss. The arithmetic mean was then calculated and this data was recorded in a table. After the last cycle and weighing of the sample, the average weight loss W_h was calculated from the measured values. After calculating the average weight loss for each sample – body of tool (basic material) and hardfacing materials – the relative resistance to abrasive wear $\Psi_{abr.}$ was calculated according to the formula:

$$\psi_{abr.} = \frac{W_{hE}}{W_{hV}} \quad (1)$$

where W_{hE} is mass loss of the comparative test body - standard [g],
W_{hV} is mass loss of the test body - sample [g].

The Table 2 lists the values of the coefficient $\Psi abr.$ - relative resistance to abrasive wear for the individual tested materials.

Table 3 Values $\Psi abr.$ - relative resistance to abrasive wear
Tabuľka 3 Hodnoty $\Psi abr.$ - relatívna odolnosť voči abrazívnemu opotrebovaniu

Material	$\Psi abr.$
Material of body tool - Steel 16CrMn5 [1)]	1
Electrode UTP BMC EN 14700	4.76
Electrode E DUR 600 EN ISO 14700	2.69
Hadfield´s steel X120Mn12 [2)]	
- Before strengthening [3)]	1.99
- After strengthening [4)]	4.00

[1)]Materiál tela nástroja, [2)]Hadfieldova oceľ, [3)]Pred spevnením, [4)]Po spevnení

The Figure 3 shows a graph of the values of the coefficient $\Psi abr.$ of individual materials.

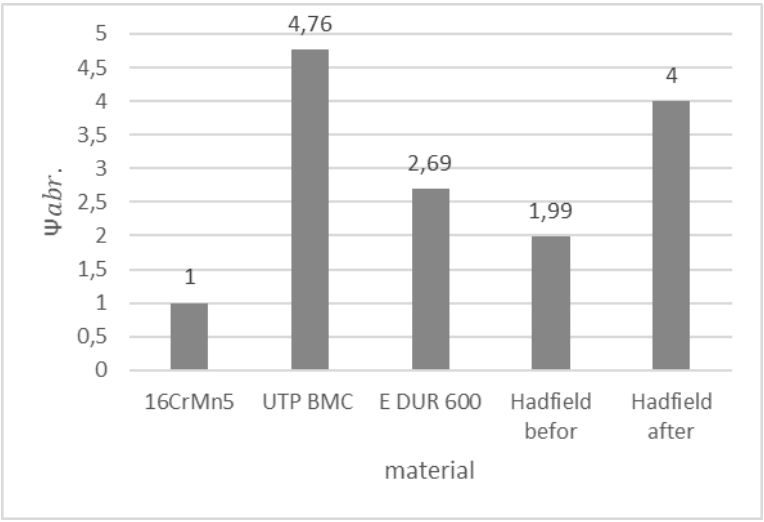

Fig. 3 Graph comparing the results of the abrasion resistance test according to GOST 23.208-79

Obr. 3 Graf, porovnávajúci výsledky skúšky odolnosti proti oteru podľa GOST 23.208-79

Evaluation of hardness and microhardness

The HRC method was chosen to evaluate hardness. HRC values are most often used in the material leaves of electrodes, which ensures a direct comparison of values.

The evaluation of HV microhardness is useful for determining the hardness of individual structural components. This mainly concerns materials that contain carbides, the hardness of which is significantly higher than the hardness of the basic ferritic matrix or eutectic. This mainly concerns hardfacing materials that contain chromium or wolfram carbides.

The hardness measurement by the HRC method of selected materials was carried out on a UH250 hardness tester, with a loading force of F= 1,471 N according to ISO 6508-1:2016. Six measurements were made on each sample and the average value was calculated from them. The results are shown in Table 4.

The hardness measurement by the HV0.1 method of selected materials was carried out on a WILSON-WOLPERT hardness tester Tukon 1102, at a load of 0.10 kp and a load application time of 15 seconds, according to EN ISO 6507. Eight measurements were made on each sample and the average value was calculated from them (Fig.4).

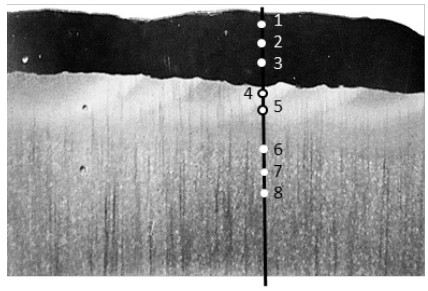

Fig. 4 Microhardness measurement HV0.1 – example Electrode E DUR 600
Obr. 4 Meranie mikrotvrdosti HV0.1 – príklad elektróda E DUR 600

The results of the measurement are shown in Table 4.

Table 4 Hardness values HRC and HV0.1
Tabuľka 4 Hodnoty vrdosti HRC a HV0.1

Material	HRC	HV 0.1
Material of body tool - Steel 16CrMn5 [1)]	18±1	283
Electrode UTP BMC EN 14700	23±1	320
Electrode E DUR 600 EN ISO 14700	61±1	960
Hadfield´s steel X120Mn12 [2)]		
- Before strengthening [3)]	30±1	320
- After strengthening [4)]	35±1	365

[1)]Materiál tela nástroja, [2)]Hadfieldova oceľ, [3)]Pred spevnením, [4)]Po spevnení

Fig. 5 and 6 show graphs of hardness values HRC (Fig. 5) and HV0.1 (Fig. 6) depending on the material under investigation.

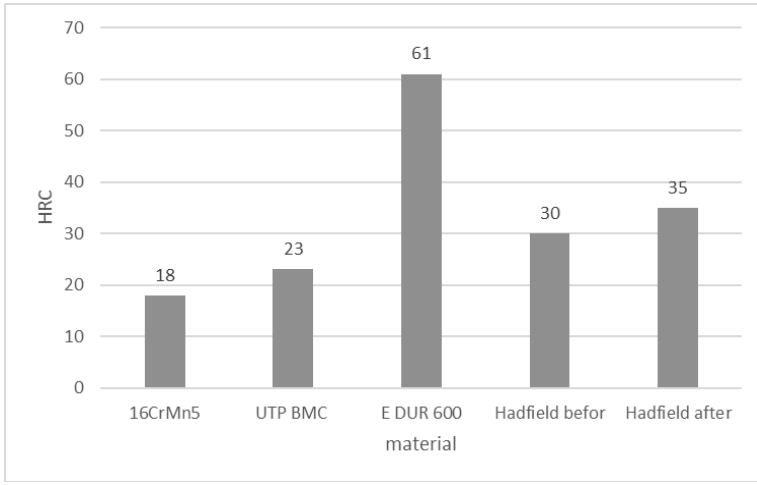

Fig. 5 Graph comparing HRC hardness values
Obr. 5 Graf porovnania hodnôt HRC

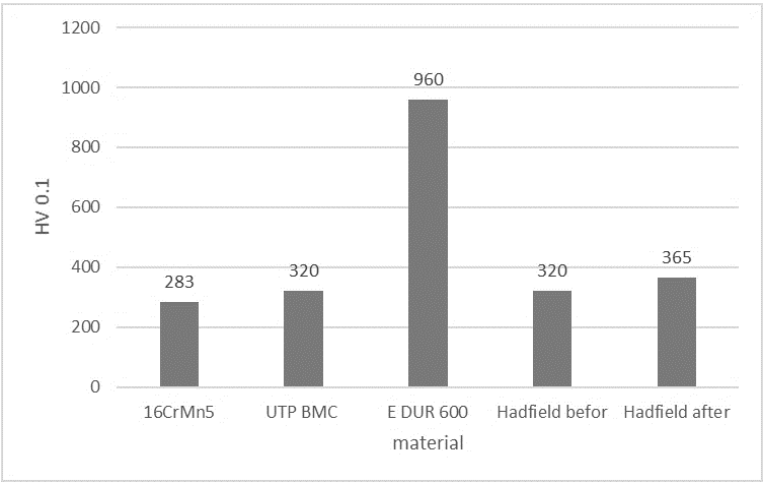

Fig. 6 Graph comparing HV0.1 hardness values
Obr. 6 Graf porovnania hodnôt HV0.1

DISCUSSION

As is evident from the results of tests and measurements, both proposed hardfacing materials achieved better abrasion resistance and higher hardness values than the base material (16CrMn5) of the tool body for the removal of unwanted growths. The same applies to Hadfield steel X120Mn12. Before and after hardening, the values of the coefficient $\Psi abr.$ - relative resistance to abrasive wear were higher than 1.

The highest coefficient $\Psi abr.$ was found for the UTP BMC electrode. Its wear resistance was almost 5 times higher. The material X120Mn12 after cold deformation strengthening came very close to it, where the wear resistance was 4 times higher. However, we can state that all four samples had values of $\Psi abr.$ higher than the base material of the tool body for crushing unwanted growths 16CrMn5.

When evaluating the hardness, a very significant HRC hardness of the E DUR 600 electrode material was recorded. It was 3.3 times higher than that of the 16CrMn5 material. The same applies to the measurement of the HV 0.1 microhardness, where the hardness of the E DUR 600 electrode material was also 3.3 times higher. We can attribute this to the higher chromium content, which forms carbides in the ferritic matrix. The hardface metal of the UTP BMC electrode also has a higher percentage of chromium, but here the higher hardness was not evident.

We can conclude that the austenitic hardfacing without strain hardening achieved higher resistance to abrasive wear than the austenitic steel after strain hardening and even higher than the ledeburitic hardfacing with twice the hardness.

Several authors for example (Balla 2003; Zum Gahr 1998; Suchánek et al. 2007; Javaheri et al. 2018; Falat et al. 2019; Singh et al. 2020) have theoretically described in their research papers the influence of factors on abrasive wear of materials. These are the influences of mechanical properties, structure, chemical elements and the influence of the abrasive (Chotěborský et al. 2009). Their influence on increasing the service life of tools, through changes in the structure of exposed parts, is evaluated through graphs in which the calculated and measured coefficients and values obtained from the results of tests and trials on samples were compared. We can state that the results achieved in the laboratory experiment largely coincide with the research results of the above authors.

CONCLUSION

Based on the measurement results, we can conclude that all three selected materials and processes increased both the hardness and abrasion resistance of the surfaces of the tools for crushing unwanted growths. The results confirm the suitability of alternative materials and techniques for improving the lifetime of tools. The hardface of the UTP BMC electrode achieved the highest wear resistance and the Hadfield steel had a significant increase in hardness after strengthening.

This can be attributed mainly to the given conditions of the structure of the applied materials, mainly due to their chemical composition and the ability to self-reinforce under operating conditions when crushing unwanted growths.

ACKNOWLEDGMENT

This work was supported by Scientific Grant Agency of the Ministry of Education, science, research and sport of the Slovak Republic and the Slovak Academy of Sciences under the grant number VEGA 1/0073/24 „Experimental analysis of shapes and materials of working tools of additional equipment of forestry mechanization technology “.

REFERENCES

BALLA, J. 2003. *Náuka o materiáloch*. Nitra: SPU, pp 168. ISBN 80-8069-249-1.

BUCHELY, M.F., GUTIERREZ, J.C., LEON, L.M. AND TORO, A. 2005. The effect of microstructure on abrasive wear of hardfacing alloys. In: *Wear*, July 259 (1), 52-61p [online] [cit. 25.07.2025]. Available on: https://www.researchgate.net/publication/228509703_The_effect_of_microstructure_on_abrasive_wear_of_hardfacing_allos DOI: 10.1016/j.wear.2005.03.002.

FALAT, L., DZUPON, M., TAVODOVA, M., HNILICA, R., LUPTACIKOVA, V., CIRIPOVA, “et al.”. 2019. Microstructure and Abrasive Wear Resistance of Various Alloy Hardfacings for Application on Heavy-Duty Chipper Tools in Forestry Shredding and Mulching Operations, In: *Materials*, July 2019 12(13): [online]. [cit. 29.07.2025]. Available on https://www.researchgate.net/publication/334380057_Microstructure_and_Abrasive_Wear_Resistanceof_Various_Alloy_Hardfacings_for_Application_on_HeavyDuty_Chipper_Tools_in_Forestry_Shredding_and_Mulching_Operations. DOI: 10.3390/ma12132212.

GOST 23.208-79 Ensuring of wear resistance of products. Wear resistance testing of materials by friction against loosely fixed abrasive particles. [online]. [cit. 25.07.2025]. Available on: http://docs.cntd.ru/document/gost-23-208-79.

HNILICA, R., MESSINGEROVÁ, V., STANOVSKÝ, M. 2015. *Possibilities of mechanization of work on forest founding and education*. (Scientific monography). pp 99. ISBN 978-80-228-2722-5.

HNILICOVÁ, M., HNILICA, R., DADO, M. 2016. Technique and technology in the upbringing and cultivation of the forest. In: *Increasing the Life of Tools and Structural Parts of Mechanisms*. Zvolen: Technická univerzita, 16–26p. ISBN 978-80-228-2862-8.

CHOTĚBORSKÝ, R. HRABĚ, P., MÜLLER, M., SAVKOVÁ, J., JIRKA, M., NAVRÁTILOVÁ, M. 2009. Effect of abrasive particle size on abrasive wear of hardfacing alloys. In: *RES. AGR. ENG.*, 55, (3): 101–113p [online]. [cit. 25.07.2025]. Available on: https://www.agriculturejournals.cz/publicFiles/10581.pdf.

ISO 6507-1:2018; Metallic Materials—Vickers Hardness Test—Part 1: Test Method. International Organization for Standardization:London, UK, 2018.

ISO 6508-1:2016; Metallic Materials—Rockwell Hardness Test—Part 1: Test Method. International Organization for Standardization: London, UK, 2018.

JAVAHERI V., PORTER, D., KUOKKALA V.T. 2018. Slurry erosion of steel – Review of tests, mechanisms and materials In: *Wear*, vol. 408–409, 248–273p. ISSN 0043-1648.

SINGH, J.C, HATHA, S.S., SIDHU, B.S. 2020. Abrasive wear behavior of newly developed weld overlaid tillage tools in laboratory and in actual field conditions. In: *Journal of Manufacturing Processes* 55, 43-152p.

SUCHÁNEK, J., KUKLÍK, V., ZDRAVECKÁ, E. 2007. *Abrazívní opotřebení materiálů*. Praha ČVUT, 2007. pp. 162. ISBN 978-80-01-03659-4.

ŤAVODOVÁ, M., HNILICOVÁ, M., MITURSKA, I. 2019. Analysis of hard facing material designed for application on the forestry tools In: *Advances in science and technology research journal*, no. 4, 111-119p. ISSN 2080-4075.

ŤAVODOVÁ, M., HNILICA, R. 2023. Possibilities of modification of tools for crushing unwanted growth and evaluation of the financial complexity of these modifications. In *Acta facultatis technicae Zvolen*, zv. 28, č. 2, 9–19p. ISSN 1336-4472.

ZUM GAHR, K.H. 1998. Wear by hard particles. In: *Tribology International*, Vol. 31, No. 10, 587-596p.

Corresponding author:
Miroslava Ťavodová, Assoc. prof., MSc., PhD., +421 5206016, tavodova@tuzvo.sk